

RESEARCH PAPER

Leaf photosynthesis and respiration of three bioenergy crops in relation to temperature and leaf nitrogen: how conserved are biochemical model parameters among crop species?

S. V. Archontoulis^{1,2}, X. Yin¹, J. Vos¹, N. G. Danalatos² and P. C. Struik^{1,*}

¹ Centre for Crop Systems Analysis, Plant Sciences Group, Wageningen University, Wageningen, The Netherlands

² Laboratory of Agronomy and Applied Crop Physiology, Department of Agriculture, University of Thessaly, Volos, Greece

* To whom correspondence should be addressed. E-mail: paul.struik@wur.nl

Received 20 June 2011; Revised 31 August 2011; Accepted 7 September 2011

Abstract

Given the need for parallel increases in food and energy production from crops in the context of global change, crop simulation models and data sets to feed these models with photosynthesis and respiration parameters are increasingly important. This study provides information on photosynthesis and respiration for three energy crops (sunflower, kenaf, and cynara), reviews relevant information for five other crops (wheat, barley, cotton, tobacco, and grape), and assesses how conserved photosynthesis parameters are among crops. Using large data sets and optimization techniques, the C₃ leaf photosynthesis model of Farquhar, von Caemmerer, and Berry (FvCB) and an empirical night respiration model for tested energy crops accounting for effects of temperature and leaf nitrogen were parameterized. Instead of the common approach of using information on net photosynthesis response to CO₂ at the stomatal cavity (A_n-C_i), the model was parameterized by analysing the photosynthesis response to incident light intensity (A_n-I_{inc}). Convincing evidence is provided that the maximum Rubisco carboxylation rate or the maximum electron transport rate was very similar whether derived from A_n-C_i or from A_n-I_{inc} data sets. Parameters characterizing Rubisco limitation, electron transport limitation, the degree to which light inhibits leaf respiration, night respiration, and the minimum leaf nitrogen required for photosynthesis were then determined. Model predictions were validated against independent sets. Only a few FvCB parameters were conserved among crop species, thus species-specific FvCB model parameters are needed for crop modelling. Therefore, information from readily available but underexplored A_n-I_{inc} data should be re-analysed, thereby expanding the potential of combining classical photosynthetic data and the biochemical model.

Key words: A_n-I_{inc} curves, acclimation, bioenergy crops, crop modelling, day and night respiration, electron transport rate, leaf nitrogen, photosynthesis, Rubisco carboxylation, temperature.

Introduction

In conventional crop modelling leaf photosynthesis is calculated from net photosynthesis light response curves (A_n-I_{inc} ; see symbols explanation in Table 1) at ambient atmospheric CO₂ level using empirical functions (e.g. SUCROS; Goudriaan and van Laar, 1994). In the context of better understanding biological processes and exploring the impact of climate change, recent crop models (e.g. GECROS; Yin and van Laar, 2005), 3D models (e.g. Evers *et al.*, 2010), or terrestrial ecosystem models (e.g. LPJmL; Beringer *et al.*, 2011) calculate photosynthesis based on the mechanistic model of Farquhar, von

Caemmerer, and Berry (Farquhar *et al.*, 1980; the FvCB model hereafter).

The FvCB model describes photosynthesis as the minimum of the Rubisco-limited rate and the electron transport-limited rate. The key parameters of the model are the maximum Rubisco carboxylation rate (V_{cmax}), the maximum electron transport rate (J_{max}), and the mitochondrial day respiration (R_d). These biochemical parameters are influenced both by the physiological status of a leaf such as the amount of leaf nitrogen per unit area (N_a) (e.g. Harley *et al.*, 1992) and by short- and long-term changes of

Table 1. List of main symbols used in this study with their definitions and units

Symbol	Definition	Unit
A_c	Rubisco-limited net photosynthetic rate	$\mu\text{mol CO}_2 \text{ m}^{-2} \text{ s}^{-1}$
A_n	Net assimilation rate	$\mu\text{mol CO}_2 \text{ m}^{-2} \text{ s}^{-1}$
A_j	Electron transport-limited net photosynthetic rate	$\mu\text{mol CO}_2 \text{ m}^{-2} \text{ s}^{-1}$
$A_{n,\text{max}}$	Light-saturated A_n	$\mu\text{mol CO}_2 \text{ m}^{-2} \text{ s}^{-1}$
a_R	x-axis intercept in Equation 12	$\mu\text{mol CO}_2 \text{ m}^{-2} \text{ s}^{-1}$
b_R	Slope parameter in Equation 12	–
C_c	CO_2 chloroplast partial pressure	μbar
C_i	Intercellular CO_2 partial pressure	μbar
D_j, D_v	Deactivation energy of J_{max} and V_{cmax} (Equation 6)	J mol^{-1}
$E_{K_{\text{mc}}}, E_{K_{\text{mo}}}$	Activation energy for K_{mc} and for K_{mo}	J mol^{-1}
E_j, E_{R_n}, E_v	Activation energy of J_{max}, R_n , and V_{cmax} (Equations 5–6)	J mol^{-1}
$E_{R_{\text{nd}}}$	Constant parameter (Equation 11)	J mol^{-1}
$E_{R_{\text{nb}}}$	Slope parameter in Equation 11	$\text{J m}^{-2} \text{ mol}^{-1} \text{ g}^{-1} \text{ N}$
g_m	Mesophyll conductance for CO_2 diffusion	$\text{mol m}^{-2} \text{ s}^{-1}$
g_s	Stomatal conductance for H_2O	$\text{mol m}^{-2} \text{ s}^{-1}$
I_{inc}	Incident light on leaf surface	$\mu\text{mol photons m}^{-2} \text{ s}^{-1}$
J	Photosystem II electron transport rate	$\mu\text{mol e}^- \text{ m}^{-2} \text{ s}^{-1}$
J_{max}	Maximum electron transport rate	$\mu\text{mol e}^- \text{ m}^{-2} \text{ s}^{-1}$
$J_{\text{max}25}$	Value of J_{max} at 25 °C	$\mu\text{mol e}^- \text{ m}^{-2} \text{ s}^{-1}$
K_{mc}	Michaelis–Menten constant for CO_2	μbar
K_{mo}	Michaelis–Menten constant for O_2	mbar
N_a	Leaf nitrogen per unit area	$\text{g N m}^{-2} \text{ leaf}$
N_b	Minimum N_a required for photosynthesis	$\text{g N m}^{-2} \text{ leaf}$
O	Oxygen partial pressure of the air (=210)	mbar
R	Universal gas constant (=8.314)	$\text{J K}^{-1} \text{ mol}^{-1}$
R_d	Day respiration rate	$\mu\text{mol CO}_2 \text{ m}^{-2} \text{ s}^{-1}$
R_n	Night respiration rate	$\mu\text{mol CO}_2 \text{ m}^{-2} \text{ s}^{-1}$
R_{n25}	Value of R_n at 25 °C	$\mu\text{mol CO}_2 \text{ m}^{-2} \text{ s}^{-1}$
S_j, S_v	Entropy term for J_{max} and V_{cmax} (Equation 6)	$\text{J K}^{-1} \text{ mol}^{-1}$
V_{cmax}	Maximum carboxylation rate	$\mu\text{mol CO}_2 \text{ m}^{-2} \text{ s}^{-1}$
$V_{\text{cmax}25}$	Value of V_{cmax} at 25 °C	$\mu\text{mol CO}_2 \text{ m}^{-2} \text{ s}^{-1}$
Γ^*	C_i -based CO_2 compensation point in the absence of R_d	μbar
θ	Convexity factor for the response of J to I_{inc}	–
κ_{2LL}	Conversion efficiency of I_{inc} into J at low light	$\text{mol e}^- \text{ mol}^{-1} \text{ photons}$
$\Phi_{\text{CO}_2\text{LL}}$	Apparent quantum yield of A_n at low I_{inc}	$\text{mol CO}_2 \text{ mol}^{-1} \text{ photons}$
χ_j	Slope of the $J_{\text{max}25}$ and N_a relationship (Equation 10)	$\mu\text{mol e}^- \text{ g}^{-1} \text{ N s}^{-1}$
χ_R	Slope of the R_{n25} and N_a relationship (Equation 8)	$\mu\text{mol CO}_2 \text{ g}^{-1} \text{ N s}^{-1}$
χ_v	Slope of the $V_{\text{cmax}25}$ and N_a relationship (Equation 9)	$\mu\text{mol CO}_2 \text{ g}^{-1} \text{ N s}^{-1}$

environmental variables such as temperature, light (e.g. Hikosaka, 2005), CO_2 (e.g. Makino *et al.*, 1994), and drought (e.g. Galmes *et al.*, 2007).

Usually, the FvCB parameters are obtained by analysis of net photosynthesis response to CO_2 at the stomatal cavity (A_n-C_i) (e.g. Sharkey *et al.*, 2007) or by combining A_n-C_i and A_n-I_{inc} curves (e.g. Braune *et al.*, 2009) or by combining these curves with chlorophyll fluorescence measurements (Yin *et al.*, 2009). Obviously, to parameterize the FvCB model, information on A_n-C_i is predominantly considered to be essential, and an ongoing discussion is mainly focused on improving the methods of analysing these A_n-C_i curves (Ethier *et al.*, 2004; Sharkey *et al.*, 2007; Gu *et al.*, 2010).

In the context of forward crop modelling typically for predictions at the ambient CO_2 level, the FvCB model is used to project leaf photosynthetic rates in response to both temporal (diurnal and seasonal) and spatial (within a crop canopy) variation in light intensity. This implies that in the context of inverse modelling, important FvCB model parameters J_{max} and V_{cmax} should and can be estimated from A_n responses to I_{inc} . This would reflect better the tradition whereby crop modellers describe leaf photosynthesis from its response to light intensity (e.g. Goudriaan, 1979), in contrast to the tradition that photosynthesis physiologists study gas exchange measurements mainly across various levels of CO_2 (e.g. von Caemmerer and Farquhar, 1981). In fact, the FvCB model can be parameterized from analysis of A_n-I_{inc} data alone (Niinemets and Tenhunen, 1997; Kosugi *et al.*, 2003), but so far there is no information about the accuracy of J_{max} and V_{cmax} parameters derived from such an analysis. If J_{max} and V_{cmax} estimates derived from analysis of A_n-I_{inc} are similar to those obtained from the common A_n-C_i analysis or combined analysis of A_n-C_i and A_n-I_{inc} curves, it may generate an opportunity to reduce empiricism in crop models by using readily available A_n-I_{inc} data. Therefore, the first objective of this study is to explore this opportunity by parameterizing the FvCB model using A_n-I_{inc} data.

In the light of current trends for a parallel increase in food and energy production from crop species in the context of climate change, the use of the FvCB-based simulation models together with an urgent need to feed these models with photosynthetic and respiration parameters has been increased (e.g. Beringer *et al.*, 2011). Compared with the rich information found for trees in the literature, there are only a few reports on J_{max} , V_{cmax} , R_d , and night respiration (R_n) parameters in relation to environmental and management factors for economically important crop species (e.g. Müller *et al.*, 2005; Braune *et al.*, 2009; Yin *et al.*, 2009) and these are virtually lacking for new bioenergy species. Therefore, the second objective of this study is 3-fold: (i) to provide new information on photosynthesis and respiration for three Mediterranean energy crops (*Helianthus annuus*, sunflower; *Hibiscus cannabinus*, kenaf; and *Cynara cardunculus*, cynara); (ii) to summarize existing information for five major cash crops (wheat, barley, cotton, tobacco, and grape); and (iii) to assess how conserved FvCB parameters are among crop species to better assist modellers in this exploitation.

Sunflower, kenaf, and cynara crops were chosen because these crops have great potential to increase bioenergy production in the Mediterranean region (Archontoulis *et al.*, 2010a, b; Danalatos and Archontoulis, 2010). In addition,

the chosen crops cover a wide range of bioindustrial applications (biodiesel, bioethanol, heat, and electricity) and fit into different cropping strategies (short or long growing period, cultivation with or without irrigation, etc.). Sunflower is widely grown in the Mediterranean region, but kenaf and cynara cultivation is still in the experimental phase; relevant information for crop modelling is currently being accumulated for these crops, including vertical distribution of light and nitrogen within crop canopies (Archontoulis *et al.*, 2011). Photosynthetic gas exchange studies for sunflower have been reported (e.g. Connor *et al.*, 1993), but there are only a few for kenaf (Muchow, 1990; Cosentino *et al.*, 2004) and none for cynara.

The present analysis focuses on the FvCB parameters in response to temperature and N_a for these bioenergy crops. This is because earlier studies on V_{cmax} and J_{max} temperature dependencies showed great species-to-species variability (Leuning, 2002; Medlyn *et al.*, 2002a), and because N_a is linearly related to Rubisco content that drives CO_2 fixation (Makino *et al.*, 1994), reflects leaf dynamics well (leaf age, rank; Archontoulis *et al.*, 2011), and comprises a reference index for scaling photosynthetic CO_2 assimilation from leaf to canopy levels (de Pury and Farquhar, 1997). Among bioenergy crops, the perennial cynara has long annual growth cycles (~10 months each; Archontoulis *et al.*, 2010a). Given the numerous reports together with their diverse findings on photosynthetic and respiratory acclimation to growth environment (Atkin *et al.*, 2005; Ow *et al.*, 2008; Yamori *et al.*, 2005, 2010; Silim *et al.*, 2010), seasonal acclimation effects on photosynthesis and respiration for the cynara crop are also investigated.

Materials and methods

Literature data for A_n-C_i versus A_n-I_{inc} curves

The first objective of this study was to compare V_{cmax} and J_{max} estimates derived either from A_n-C_i or from A_n-I_{inc} curves. For this, published data from Yin *et al.* (2009) for *Triticum aestivum* (cv. Minaret) were used. All relevant parameter values required to fit the FvCB model to the A_n-C_i or A_n-I_{inc} data set were available, therefore avoiding any statistical artefact in V_{cmax} and J_{max} estimation. Wheat measurements (four replicates; all at 25 °C) were conducted on leaves with different N_a status (15 sets of A_n-C_i and 15 of A_n-I_{inc} curves), allowing the comparison of J_{max} and V_{cmax} estimates to be made over a wide range of their values. For more information about the measurements, see Yin *et al.* (2009).

Energy crop species and study site

Sunflower (cv. Panter), kenaf (cv. Everglades 41), and cynara (cv. Biango avorio) crops were grown in different sections of the same field (for details, see Archontoulis *et al.*, 2011) in central Greece (39°25'43.4" N, 22°05'09.7" E, 105 m asl) for 3 years (2007–2009). The site has a Mediterranean climate with cold/wet winters and warm/dry summers (Supplementary Fig. S1 available at *JXB* online). The soil was loamy, classified as Aquic Xerofluvent, with a shallow groundwater table (1.8–2.8 m below the surface during May). In general, crops grown at that site produce much higher biomass yields than crops grown on dry soils (e.g. Archontoulis *et al.*, 2010b). During summer, sunflower and kenaf crops were frequently irrigated at intervals of 4–6 d according to potential evapotranspiration (for site-specific calculations, see Danalatos and

Archontoulis, 2010) while cynara was irrigated only a few times, when necessary during May–June but not during November–April (see precipitation in Supplementary Fig. S1).

Gas exchange measurements and experimental protocol

Leaf gas exchange (GE) measurements were implemented *in situ* in fully expanded leaves using a portable open gas exchange system with a 6.25 cm² clamp-on leaf chamber (ADC, LCI/LCpro+, Bioscientific Ltd, Hoddesdon, UK). CO_2/H_2O exchanged by the leaf was measured using an infrared gas analyser in a differential mode. The system allowed for an automated microclimate control in the leaf chamber. Before each measurement, attached leaves were adapted for 10–45 min to chamber conditions, depending on leaf age, time of the day, and season. Daytime GE measurements were taken within 1–2 d after irrigation and during morning hours to ensure no water stress and to avoid midday depression of photosynthesis. Night-time GE measurements were initiated 30–45 min after sunset and lasted for 4–5 h each time.

To parameterize the model, a common experimental protocol was applied per species, including four different sets of GE measurements. In all sets, CO_2 concentration was kept at $380 \pm 5 \mu\text{mol mol}^{-1}$. The first set aimed to determine the response of net photosynthesis (A_n) to incident light (I_{inc}). Accordingly, at fixed leaf temperature and measured N_a , A_n was determined in 11 I_{inc} steps (2000, 1500, 1000, 500, 250, 200, 150, 100, 50, 20, and 0 $\mu\text{mol photons m}^{-2} \text{s}^{-1}$); in total, 76 curves were constructed. Adaptation time to each I_{inc} level was ~5 min, except for $I_{inc}=0$ where it was >10 min; 3–5 replicated A_n measurements were taken at each I_{inc} step to ensure stability and precision of measurements. Given that the examination of steady-state photosynthesis takes considerable time and that GE measurements should be done within a limited time frame in order to avoid stress conditions (see above), the response of A_n to leaf temperature (set II) was determined at three I_{inc} levels: 450, 900, and 1800 $\mu\text{mol photons m}^{-2} \text{s}^{-1}$. N_a was also determined. At each I_{inc} , leaf temperature was increased or decreased up to 10 °C from the ambient temperature in steps of 2–4 °C and replicated A_n measurements were recorded every 5 min. To establish the relationship between net photosynthesis and N_a (set III), it was necessary to evaluate leaves with as wide an N_a range as possible. So, in addition to earlier sets, A_n measurements were done at saturated I_{inc} (1600–1800 $\mu\text{mol photons m}^{-2} \text{s}^{-1}$) on leaves from different insertion heights in the canopy, from different growth stages, and from plots with different N status. Per leaf (~180 leaves assessed), 5–10 measurements were taken at leaf temperature close to the ambient temperature.

To obtain direct measurements of the mitochondrial respiration occurring in the night (R_n), the response of R_n to temperature was investigated (set IV). Leaf temperature increased or decreased up to 10 °C from the ambient temperature in small steps of 1–2 °C, and replicated R_n measurements were recorded every 4 min. Measurements were done on leaves with (as much as possible) variable N_a .

To validate the models, GE measurements obtained from the same genotypes growing in the same site during summer 2005 and 2006 (set V) were used. Sunflower and kenaf GE measurements were collected using similar techniques and time frames to those described for sets I–IV. In cynara, a different protocol was followed. The external unit that controls chamber microclimate was removed to obtain measurements under real ambient conditions. Measurements were recorded every 4–8 min, while climatic variables were continuously changing following 24 diurnal trends, thereby providing a data set to assess whether the FvCB model can predict A_n under real fluctuating field conditions.

The wide range of measuring temperature used (15–40 °C) unavoidably resulted in variation in vapour pressure difference (VPD). An effort was made to reduce that variation by keeping humidity high at high temperature. In most cases, VPD was maintained below 3 kPa to prevent stomatal closure (Bernacchi *et al.*, 2001). Although VPD was sometimes above 3 kPa at the

highest temperatures, the stomatal conductance for H₂O vapour was not less than 0.30 mol m⁻² s⁻¹ (as in Yamori *et al.*, 2005).

All measured A_n data were corrected for the CO₂ respired under the gasket surface (total 4 mm width; R. Newman, personal communication) following the common approach of Pons and Welschen (2002). All GE characteristics were re-calculated according to von Caemmerer and Farquhar (1981), for example to provide the C_i values that are required as input to the FvCB model (see below). In addition, the number of replications and observations were increased to reduce the measurement noise, especially when low CO₂ exchange rates were measured (e.g. respiration).

The portion of the leaf used for measurements was cut and its area was measured with a Li-Cor area meter. The leaf material was then weighed after drying at 70 °C to constant weight and its total nitrogen concentration was measured using the Kjeldahl method. From these measurements, the leaf nitrogen content N_a (g N m⁻²) was calculated.

Model and its parameterization

The FvCB model predicts A_n (μmol CO₂ m⁻² s⁻¹) as the minimum of two processes (see Fig. 1), the Rubisco carboxylation-limited rate (A_c) and the RuBP regeneration- or electron transport-limited rate (A_j):

$$A_n = \min(A_c, A_j) \quad (1)$$

Rubisco-limited photosynthesis is calculated as a function of maximum carboxylation capacity (V_{cmax} , μmol CO₂ m⁻² s⁻¹):

$$A_c = \frac{V_{cmax}(C_i - \Gamma_*)}{C_i + K_{mc}(1 + O/K_{mo})} - R_d \quad (2)$$

where C_i (μbar) and O (mbar) are the intercellular partial pressures of CO₂ and O₂, respectively, K_{mc} (μbar) and K_{mo} (mbar) are the Michaelis–Menten coefficients of Rubisco for CO₂ and O₂, re-

spectively, and Γ_* (μbar) is the CO₂ compensation point in the absence of R_d (day respiration in μmol CO₂ m⁻² s⁻¹, which comprises mitochondrial CO₂ release occurring in the light other than photorespiration; von Caemmerer *et al.*, 2009).

There are various equations to describe the rate of photosynthesis when RuBP regeneration is limiting (Farquhar and von Caemmerer, 1982; Yin *et al.*, 2004). The most widely used form is given by:

$$A_j = \frac{J(C_i - \Gamma_*)}{4C_i + 8\Gamma_*} - R_d \quad (3)$$

where J (μmol e⁻ m⁻² s⁻¹) is the photosystem II electron transport rate that is used for CO₂ fixation and photorespiration. J is related to the amount of incident photosynthetically active irradiance (I_{inc} ; μmol photons m⁻² s⁻¹) by:

$$J = \frac{\left(\kappa_{2LL} I_{inc} + J_{max} - \sqrt{(\kappa_{2LL} I_{inc} + J_{max})^2 - 4\theta J_{max} \kappa_{2LL} I_{inc}} \right)}{2\theta} \quad (4)$$

where J_{max} (μmol e⁻ m⁻² s⁻¹) is the maximum electron transport rate at saturating light levels, θ is a dimensionless convexity factor for the response of J to I_{inc} , and κ_{2LL} (mol e⁻ mol⁻¹ photons) is the conversion efficiency of I_{inc} into J at limiting light levels (Yin and Struik, 2009a; Yin *et al.*, 2009). The formulation of Equations 2 and 3 assumes infinitive mesophyll conductance (g_m) for CO₂ transfer to chloroplasts, so that C_i is used as the proxy for the chloroplast CO₂ level (C_c). There is increasing evidence that g_m might be low enough to allow a significant drawdown of C_c from C_i in most species (Warren, 2004; Flexas *et al.*, 2008). However based on the available GE data, it was risky to evaluate g_m (Pons *et al.*, 2009; von Caemmerer *et al.*, 2009; Yin and Struik, 2009b), hence the forms of Equations 2 and 3 had to be used, as in most earlier studies (e.g. Medlyn *et al.*, 2002a; Kosugi *et al.*, 2003). Omitting g_m in the analysis means

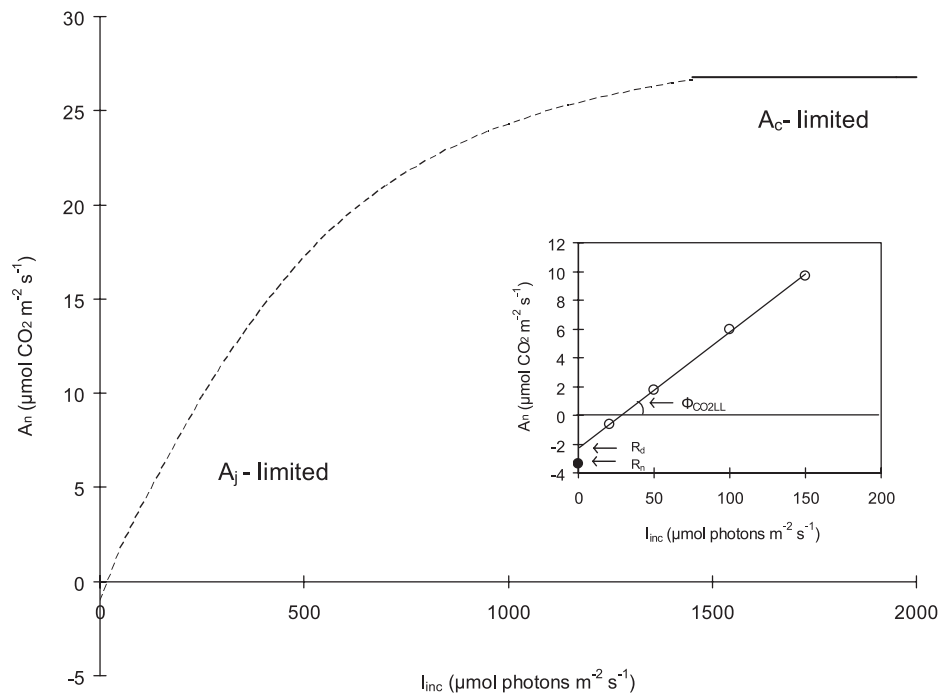


Fig. 1. Main panel: typical net photosynthesis light response curve (A_n - I_{inc}) at ambient CO₂ concentration. Curve regions for the Rubisco carboxylation-limited rate (A_c -limited, Equation 2; solid line) and the electron transport-limited rate (A_j -limited, Equation 3; dotted line) are indicated. Usually, A_c -limitation occurs above 1500 μmol photons m⁻² s⁻¹; however, it is also possible that the entire A_n - I_{inc} curve is described as A_j -limited. Inset panel: representative portion of the A_n - I_{inc} curve used in calculations of the day respiration (R_d), night respiration (R_n), and apparent quantum yield (Φ_{CO2LL}). R_d and Φ_{CO2LL} were calculated from linear regression analysis to open circles while the filled circle represents the value of the R_n . For details, see the Materials and methods.

that an appropriate consideration is needed in choosing values of the Rubisco kinetic constants (see below).

The temperature responses of respiration and of Rubisco kinetic properties (K_{mc} and K_{mo}) are described using an Arrhenius function (Equation 5) while the temperature responses of V_{cmax} and J_{max} were explored using a peaked Arrhenius function (Equation 6); both functions were normalized with respect to their values at 25 °C:

$$X = X_{25} \exp \left[\frac{E_x(T - 25)}{298R(T + 273)} \right] \quad (5)$$

$$X = X_{25} \exp \left[\frac{E_x(T - 25)}{298R(T + 273)} \right] \cdot \left[\frac{1 + \exp \left(\frac{298S_x - D_x}{298R} \right)}{1 + \exp \left(\frac{(T + 273)S_x - D_x}{R(T + 273)} \right)} \right] \quad (6)$$

where T is the leaf temperature (°C); X_{25} is the value of each parameter at 25 °C (R_{n25} , K_{mc25} , K_{mo25} , V_{cmax25} , and J_{max25}); E_x is the activation energy of each parameter (E_{R_n} , $E_{K_{mc}}$, $E_{K_{mo}}$, E_v , and E_j ; in J mol⁻¹); D_x is the deactivation energy for J_{max} and V_{cmax} (D_j and D_v in J mol⁻¹); S_x is the entropy term for J_{max} and V_{cmax} (S_j , S_v in J K⁻¹ mol⁻¹), and R is the universal gas constant (=8.314 J K⁻¹ mol⁻¹). Given that Equation 5 is a special case of Equation 6, F -tests were performed to determine whether Equation 6 described temperature responses of V_{cmax} and J_{max} significantly better than did Equation 5. When Equation 6 was overparameterized, as often observed in the literature (Dreyer *et al.*, 2001; Medlyn *et al.*, 2002a), then S_x was fixed at 650 J K⁻¹ mol⁻¹ (Harley *et al.*, 1992).

Rubisco kinetic properties are generally assumed constant among C₃ species (von Caemmerer *et al.*, 2009). However, values of these constants and their temperature dependency reported in the literature vary appreciably, so the choice of Rubisco parameters is a matter of considerable uncertainty (Dreyer *et al.*, 2001). In this work, similar to many other reports (e.g. Medlyn *et al.*, 2002a; Müller *et al.*, 2005), Rubisco parameters reported by Bernacchi *et al.* (2001) were selected because these values (i) were estimated from *in vivo* measurements without disturbance of the leaf; and (ii) were derived using the C_i-based FvCB model and hence are compatible with the present analysis assuming an infinite g_m (see above). The parameter values are: $K_{mc25}=404.9$ μbar; $K_{mo25}=278.4$ mbar; $E_{K_{mc}}=79\,430$ J mol⁻¹; and $E_{K_{mo}}=36\,380$ J mol⁻¹ (Table 1). Furthermore, using these values, the temperature dependence of Γ^* was calculated as (Yin *et al.*, 2004):

$$\Gamma^* = 0.50 \frac{K_{mc}}{K_{mo}} \left[\exp \left(-3.3801 + \frac{5220}{298R(T + 273)} \right) \right] \quad (7)$$

where the factor 0.5 is mol CO₂ released when Rubisco catalyses the reaction with 1 mol O₂ in photorespiration. The term in the brackets was derived using Bernacchi *et al.* (2001) parameters for temperature dependence of maximum carboxylation and oxygenation rates of Rubisco.

The basal capacity of R_{n25} , V_{cmax25} , and J_{max25} is linearly related to N_a (Harley *et al.*, 1992; Hirose *et al.*, 1997; Müller *et al.*, 2005; Braune *et al.*, 2009):

$$R_{n25} = \chi_R(N_a - N_b) \quad (8)$$

$$V_{cmax25} = \chi_v(N_a - N_b) \quad (9)$$

$$J_{max25} = \chi_j(N_a - N_b) \quad (10)$$

where χ_R (μmol CO₂ g⁻¹ N s⁻¹), χ_v (μmol CO₂ g⁻¹ N s⁻¹), and χ_j (μmol e⁻ g⁻¹ N s⁻¹) are the slopes for R_{n25} , V_{cmax25} , and J_{max25} , respectively, and N_b (g N m⁻²) is the minimum value of N_a at or below which A_n is zero. In principle, this N_b is practically impossible to measure and its estimation depends on the statistical methods used and on the available data sets. For instance, different N_b estimates were found when different data sets were examined (A_n or

V_{cmax} , or J_{max} ; e.g. Harley *et al.*, 1992; Müller *et al.*, 2005; Supplementary Table S1 at JXB online) or when N_b was estimated simultaneously with other parameters in optimization procedures or when different equations (linear or non-linear) were applied to the same data set (Niinemets and Tenhunen, 1997). Given the simplicity required in modelling and the lack of biological interpretation of different N_b values for the same species, a unique N_b value (per species) was determined beforehand from direct assessments of A_n - N_a plots. Then this estimate was used as input parameter.

There is some evidence that the activation energy for respiration (E_{R_n}) depends on the position of the leaf in the canopy (Bolstad *et al.*, 1999; Griffin *et al.*, 2002) and perhaps E_{R_n} is also associated with N_a since a close relationship between leaf canopy position and N_a usually exists (Archontoulis *et al.*, 2011). This was tested by assuming a linear relationship between E_{R_n} and N_a :

$$E_{R_n} = E_{R_{n(a)}} + E_{R_{n(b)}} N_a \quad (11)$$

and it was checked whether the slope parameter $E_{R_{n(b)}}$ differed significantly from zero.

So far, temperature and nitrogen relationships for R_n have been described, as extensive GE measurements during the night period were available. However, the FvCB requires estimates for R_d , which is much more difficult to measure. To estimate R_d , regression analysis was applied to the linear sections of the A_n - I_{inc} curves for each species (Fig. 1, inset; Kok method; Sharp *et al.*, 1984). From this analysis, R_d was calculated as the y -axis intercept of the linear regression and the corresponding R_n was estimated as the mean of the A_n values at 0 μmol photons m⁻² s⁻¹. Additionally, the apparent quantum efficiency at limiting light (Φ_{CO2LL} , mol CO₂ mol⁻¹ photons) on the incident light basis was calculated from the slope of the regression. The I_{inc} range for this regression analysis was typically 20–150 μmol m⁻² s⁻¹ (Fig. 1, inset), while in a few cases the I_{inc} range was slightly different, especially for data sets obtained at high temperatures. The estimated R_d was then related to R_n as:

$$R_d = b_R \times (R_n - a_R) \quad (12)$$

where b_R and a_R are the slope and the x -axis intercept of the linear model, respectively. By assuming that activation energies for R_d and R_n are similar and taking into account the precise quantification of R_n based on a large data set, the temperature and nitrogen dependencies of R_d can be calculated from combining Equations 5, 8, 11, and 12. This approach allows R_d values to be estimated for sets II and III (see above) where I_{inc} exceeds 350 μmol m⁻² s⁻¹, for which it was not possible to use the Kok method for estimating R_d .

Summary of parameters and statistics

The basic equations of the FvCB model, Equations 1–4, capture the response of A_n to C_i and to I_{inc} . Coupled with auxiliary temperature (Equations 5–7) and nitrogen (Equations 8–12) equations, the model also quantifies leaf photosynthesis and respiration (R_d and R_n) in response to these environmental variables. Data from sets I–IV were analysed using step-wise optimization procedures. Per crop, 16 parameters were estimated following the order: step 1, N_b ; step 2, χ_R , $E_{R_{n(a)}}$, $E_{R_{n(b)}}$; step 3, b_R , a_R ; step 4, χ_v , E_v , D_v , S_v ; step 5, κ_{2LL} ; step 6, χ_j , E_j , D_j , S_j , and θ (see the Results). Inputs to the model are: C_i , I_{inc} , leaf temperature, and N_a . So, just like using A_n - C_i curves, using A_n - I_{inc} data to calculate FvCB model parameters (e.g. V_{cmax}) also requires C_i as an input to the model, meaning that any (short-term) change in stomatal aperture during the A_n - I_{inc} measurements will have been reflected in the values of C_i and thus have little effect on the calculation of the FvCB parameters. For a similar reason, the direction of changing I_{inc} levels for measuring A - I_{inc} curves will also have little impact on parameter estimation (see Yin *et al.*, 2011).

For each step, regression fitting was carried out using the GAUSS method in PROC NLIN of SAS (SAS Institute Inc.) to investigate seasonal effects of acclimation on photosynthesis and

respiration rates of cynara, data sets were split into two periods: a cold period with low light from November to April and a warm period with high light from May to June (Supplementary Fig. S1 at *JXB* online). Then, dummy variables ($Z1=1$ and $Z2=0$ for warm and $Z1=0$ and $Z2=1$ for cold periods, respectively) were introduced into the regression analysis to separate for the effects. A dummy variable was also used to best estimate the N_b parameter (see the Results).

The goodness of model fit was assessed by calculating r^2 and the relative mean root square error ($rRMSE$). A sensitivity analysis was also performed. Model predictions were validated against independent data sets (set V).

Results

V_{cmax} and J_{max} estimates from A_n-C_i and/or A_n-I_{inc} curves

V_{cmax} and J_{max} were estimated for wheat, from either A_n-I_{inc} or A_n-C_i curves alone or from the combined data of the two curves. The following parameters were set as inputs to the model (see Equations 1–4 and 7): K_{mc25} and K_{mo25} from Bernacchi *et al.* (2001); and R_{d25} , R_{n25} , κ_{2LL} , and θ per set of data from Yin *et al.* (2009). V_{cmax} and J_{max} were successfully estimated simultaneously in 40 out of the 45 cases (15 sets \times 3 methodologies). In five cases, it was not possible to estimate V_{cmax} from A_n-I_{inc} curves because in these cases the entire curve was A_j limited (Fig. 1). Then we first calculated V_{cmax} directly from Equation 2 with observed C_i as input for simple substitution using data points where $I_{inc} > 1500 \mu\text{mol photons m}^{-2} \text{s}^{-1}$, and secondly by setting V_{cmax} as an input to the model, the J_{max} parameter was estimated again. To be consistent, results for all A_n-I_{inc} curves were presented following the two-step approach, because estimates from both approaches were very close.

Figure 2 illustrates V_{cmax} and J_{max} estimates from A_n-C_i and from A_n-I_{inc} curves versus the combination of those curves. As expected, V_{cmax} and J_{max} estimates obtained from A_n-C_i curves were almost identical to the estimates based on the combined data ($r^2=0.97-0.99$). However, it was found that A_n-I_{inc} curves alone also provided sufficient estimates ($r^2=0.91-0.93$) and thus can be considered as an alternative to predominant A_n-C_i curves to parameterize the FvCB

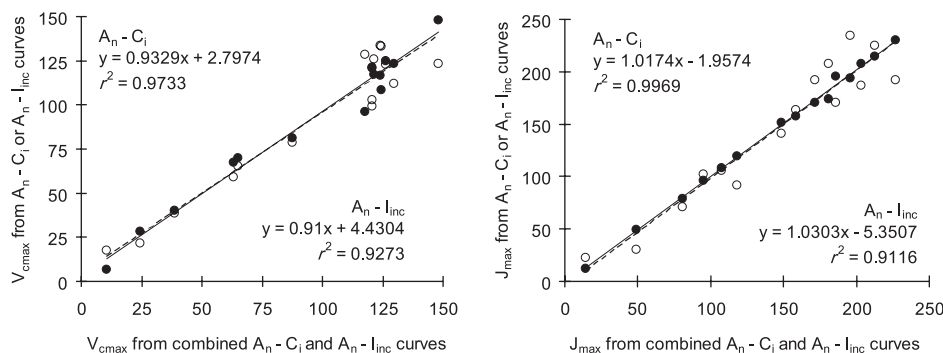


Fig. 2. Relationships between V_{cmax} ($\mu\text{mol CO}_2 \text{ m}^{-2} \text{ s}^{-1}$) and J_{max} ($\mu\text{mol e}^- \text{ m}^{-2} \text{ s}^{-1}$) estimated from photosynthetic light response curves at ambient CO_2 concentration (open circles; A_n-I_{inc}) or from photosynthetic CO_2 response curves at saturated light (filled circles; A_n-C_i) versus estimates obtained from an analysis of combined A_n-I_{inc} and A_n-C_i curves. Data for A_n-C_i and A_n-I_{inc} measurements are from Yin *et al.* (2009) for *Triticum aestivum* ($n=15$).

model. In fact, regression lines in Fig. 2 were matching across a very wide range of V_{cmax} and J_{max} values. Even in cases where photosynthetic responses to light were entirely A_j limited (Fig. 1), V_{cmax} estimates obtained from either A_n-I_{inc} or A_n-C_i data were close (Fig. 2). The slight discrepancy of the estimates at high V_{cmax} and J_{max} values (Fig. 2) caused a lower r^2 for the A_n-I_{inc} compared with the A_n-C_i estimates.

Step-wise estimation of model parameters for bioenergy crops

Step 1: N_b estimation

Measured light-saturated A_n ($A_{n,max}$) responded non-linearly to increasing N_a in all tested crops (Fig. 3; $r^2 > 0.81$; $P < 0.001$). An effect of temperature was detected in this relationship only at high N_a (Fig. 3). To estimate the N_b value properly from these plots a dummy variables approach was used, in order to obtain a unique N_b estimate per crop, while allowing the equation to vary with different temperatures (optimum versus non-optimum temperature ranges; Fig. 3). Derived parameters are listed in Table 2. N_b values for all crops were close to 0.4 g N m^{-2} , while the lack of N_a data below 0.7 g m^{-2} caused a high standard error of the N_b estimate (Table 2).

Step 2: R_n in relation to temperature and N_a

By combining Equations 5, 8, and 11, R_n parameters were estimated (Table 3). In cynara, an additional seasonal effect was found, with significantly higher R_n rates for the winter/cold- compared with the summer/warm-growing leaves (Fig. 4). Incorporation of this effect into the model improved r^2 from 0.68 to 0.72. Of the two R_n parameters, temperature sensitivity (E_{Rn}) was significantly ($P < 0.01$) affected by season, but the slope of the R_n-N_a relationship (χ_R) was not ($P=0.263$); thus, a common χ_R value was calculated (Table 3). The R_n models' goodness of fit was satisfactory ($r^2 > 0.72$; $rRMSE < 0.28$ across species).

Step 3: relationship between R_d and R_n

Plotting R_d versus R_n gave a good linear relationship with no significant differences among species ($P=0.225$; Fig. 5;

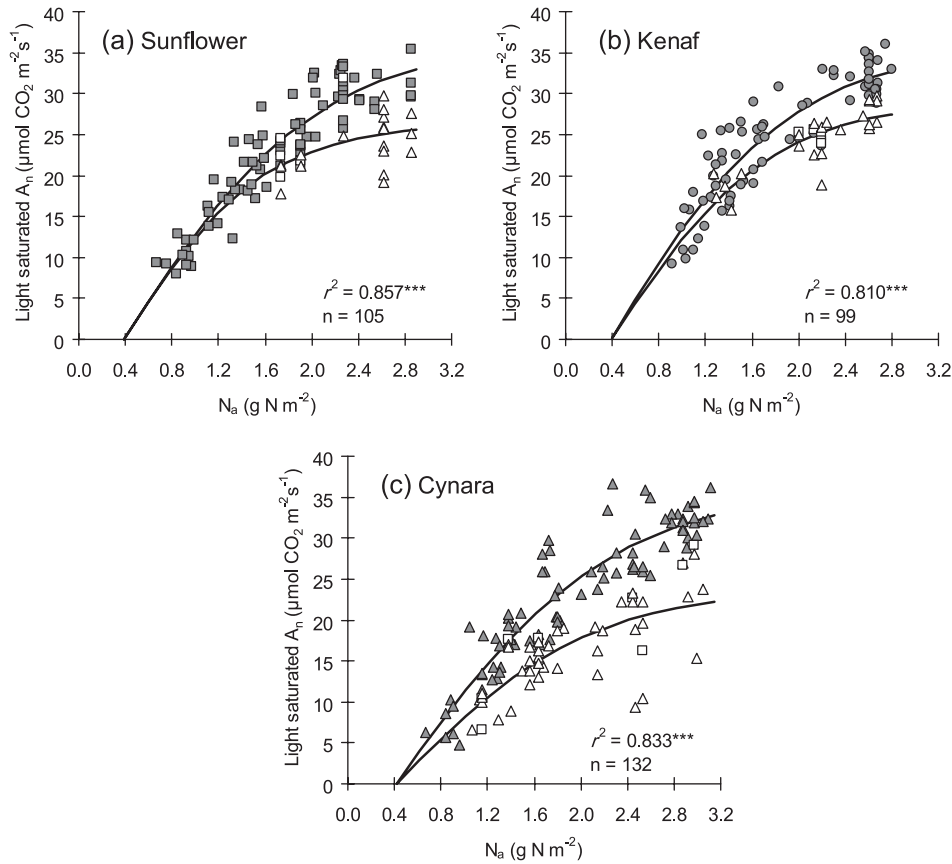


Fig. 3. Relationships between light-saturated net photosynthesis, A_n ($I_{inc} > 1500 \mu\text{mol m}^{-2}\text{s}^{-1}$; $\text{CO}_2 = 380 \mu\text{mol mol}^{-1}$), and leaf nitrogen content, N_a . Filled symbols refer to data obtained at temperatures near the optimum temperature for photosynthesis per species (sunflower, 26–34 °C; kenaf, 27–35 °C; cynara, 23–31 °C) and open symbols refer to data obtained at sub- (open squares) or supra- (open triangles) optimum temperature ranges. Each point is an average of 4–10 measurements. Lines are fits from a three-parameter non-linear equation: $A_n = A_{n,max} \{2/[1 + \exp(-c(N_a - N_b))]\} - 1$, (see Sinclair and Horie 1989), where $A_{n,max}$ is the asymptote (maximum value) of the dependent variable; c is the parameter determining the steepness of the curve; and N_b is the intercept of the x-axis denoting a threshold leaf nitrogen value at or below A_n equals zero. Estimates of parameters are given in Table 2. Cynara's data points were mostly collected during May–June.

Table 2. Estimates (SE in parentheses) of the non-linear equation used to describe data illustrated in Fig. 3

$A_{n,max}$ is the maximum net assimilation rate ($\mu\text{mol CO}_2 \text{m}^{-2} \text{s}^{-1}$) at saturated light, maximal leaf nitrogen content, ambient CO_2 concentration, and at optimum (filled symbols) and non-optimum (open symbols) temperature ranges; c is a dimensionless factor determining the steepness of the non-linear model; and N_b is the minimum leaf nitrogen content (g N m^{-2}) required for photosynthesis.

Species	Symbol ^a	$A_{n,max}$	c	N_b ^b
Sunflower	Filled (26–34 °C)	36.6 (2.48)	1.19 (0.195)	0.387 (0.078)
	Open	26.4 (1.45)	1.65 (0.313)	
Kenaf	Filled (27–35 °C)	35.8 (2.18)	1.29 (0.269)	0.390 (0.126)
	Open	29.2 (2.12)	1.45 (0.334)	
Cynara	Filled (22–31 °C)	36.4 (2.41)	1.08 (0.191)	0.416 (0.097)
	Open	23.9 (2.16)	1.22 (0.725)	

^a Symbols in Fig. 3.

^b The confidence limits for N_b are: 0.231–0.541, 0.139–0.640, and 0.225–0.608 for sunflower, kenaf, and cynara, respectively ($P=0.05$).

Table 3). Analysis showed that mitochondrial respiration was inhibited by ~28% in the light. The observed x-axis intercept ($a_R=0.39$) differed significantly from zero

($P=0.0039$), indicating that R_n and R_d were not entirely proportional (Fig. 5). Additionally, no effect of N_a ($r^2=0.01$; $P=0.67$) but a significant effect of temperature ($r^2=0.18$; $P=0.008$) was found on the R_d/R_n ratio, showing that the ratio approached unity at high temperatures. Similarly, the $R_n/A_{n,max}$ ratio—ranging from 7% to 11% across bioenergy species—was insensitive to changes in N_a ($P > 0.05$), but increased significantly with increasing temperature ($r^2=0.62$; $P < 0.01$; data not shown).

Step 4: V_{cmax} in relation to temperature and N_a

The relationships of V_{cmax} to temperature and N_a were quantified by fitting Equations 2 and 5–12 to data obtained at high light levels ($I_{inc} \geq 1500 \mu\text{mol m}^{-2} \text{s}^{-1}$) to ensure that A_n is limited only by Rubisco. All required parameters (χ_v , E_v , D_v , and S_v) were well estimated. Across species, there were small differences in χ_v (<12%; Table 3), and large differences in temperature sensitivities >30 °C (Fig. 6a; including other crops). Sunflower temperature sensitivity was best described by the peaked Arrhenius equation ($r^2=0.736$; $P < 0.001$; Table 3), showing an optimum

Table 3. Estimates (SE in parentheses) of parameters used to describe temperature and nitrogen sensitivities of photosynthesis and respiration rates in three bioenergy crops

For cynara, when significant differences between warm and cold seasons were found, two estimates are given. For units see Table 1.

	Parameter	Sunflower	Kenaf	Cynara-warm ^a	Cynara-cold ^a
R_n	χ_R	0.609 (0.006)	0.954 (0.015)	0.775 (0.009)	
	$E_{R_{(nb)}}$	117 912 (1814)	100 740 (3250)	-10 900 (5617)	146 956 (4281)
	$E_{R_{(nb)}}$	-23 346 (770)	-15 743 (1455)	33 040 (2490)	-26 640 (1858)
	n (night) ^b	2492	1403	3212	
	r^2	0.799	0.793	0.724	
R_d/R_n	b_R		0.843 (0.040)		
	a_R		0.390 (0.107)		
V_{cmax}	χ_v	73.8 (0.94)	66.7 (0.92)	65.2 (0.62)	
	E_v	53 688 (1631)	61 812 (1402)	190 831 (33 853)	
	D_v	205 638 (355)	0	158 486 (30 907)	
	S_v	650 ^c	0	550 (108.2)	
J	χ_j	144.2 (3.4)	122.1 (1.88)	100 (0.91)	92.2 (0.88)
	E_j	43 295 (5122)	28 584 ^d (1131)	23 111 (971)	
	D_j	125 324 (12 653)	0 ^d	204 489 (218)	
	S_j	405 (38.47)	0 ^d	650 ^c	
	κ_{2LL}	0.255 (0.018)	0.278 (0.013)	0.314 (0.014)	0.419 (0.011)
	θ	0.607 (0.027)	0.627 (0.023)	0.847 (0.011)	
	n (day) ^b	1366	2042	2334	
	r^2	0.928	0.909	0.916	
	Ratio	J_{max}/V_{cmax}^e	1.95	1.83	1.53
	R_d/V_{cmax}^e	0.0057	0.0103	0.0085	

^a Warm period=from early May to end of June; cold period=from November to mid-April; see supplementary Fig. S1 at JXB online.^b Number of data used in the analysis.^c Fixed value (see the Materials and methods).^d Alternatively the following parameters: $E_j=28\ 149$, $D_j=474\ 614$, and $S_j=1482$ (with a temperature optimum of 41.7 °C) gave equal temperature sensitivities but values were rejected due to a high standard error of the estimate.^e Normalized to 25 °C.

temperature for V_{cmax} at 38.7 °C (calculated from Equation A1 in the Appendix). For kenaf and cynara no optimum temperature was observed within the measurement range tested (18–41 °C; Fig. 6a). To explore any acclimation of V_{cmax} to growth environments in cynara, the model was allowed to estimate different parameters for two contrasting seasons. No significant effect of the growing season on χ_v (65.8 versus 64.3; $P=0.094$) or on E_v , D_v , and S_v parameters ($P=0.247$) was found, meaning little seasonal V_{cmax} acclimation.

Step 5: κ_{2LL} in relation to temperature and N_a

κ_{2LL} was estimated indirectly from Φ_{CO2LL} information (see Equation A2). Correlations of κ_{2LL} with temperature, light, and nitrogen were investigated afterwards. The results indicated poor correlations with N_a ($r^2=0.26$, $P=0.025$), leaf temperature ($r^2=0.19$, $P=0.104$), and the combination of the above ($r^2=0.44$, $P < 0.01$; data not shown). However, better relationships were obtained when κ_{2LL} was regressed against seasonal temperature ($r^2=0.40$, $P=0.004$) and radiation data ($r^2=0.34$, $P=0.003$), showing a long-term κ_{2LL} acclimation. This became clearer when average κ_{2LL} values per crop and per growth environments were considered (Fig. 7). These findings were supported fairly well by literature data (Fig. 7). Based on this analysis, average κ_{2LL} values per species were considered in further analyses (including acclimation effect for cynara, Table 3).

Step 6: J_{max} in relation to temperature and N_a

All J_{max} temperature sensitivities (except kenaf; Table 3) were best described using Equation 6. Across species, J_{max} temperature sensitivity was highly variable (Fig. 6b including other crops), while the maximum J_{max} was obtained at lower temperature than the maximum V_{cmax} (temperature optimum of 32, 42, and 33 °C for sunflower, kenaf, and cynara, respectively; Fig. 6). As a result, there was a decreasing trend of the J_{max}/V_{cmax} ratio with increasing temperature (Fig. 8). For cynara, a significant ($P < 0.05$) temporal change was found for the χ_j parameter (Table 3). χ_j showed a larger variability (36% change) than χ_v (12% change) among species and growth environments studied (Table 3). The parameter θ was lower for sunflower (0.60) and higher for cynara (0.84), but close to the commonly used value of 0.75 in all cases. All these differences (including temperature and nitrogen sensitivities) among species and growth environments became smaller when the J_{max}/V_{cmax} ratio was plotted against leaf temperature (Fig. 8).

Sensitivity and validation analysis

To investigate the uncertainty introduced into the estimates by the chosen Rubisco kinetic parameters, the initial values of Bernacchi et al. (2001) were increased or decreased by 20% and optimization procedures were repeated. Not

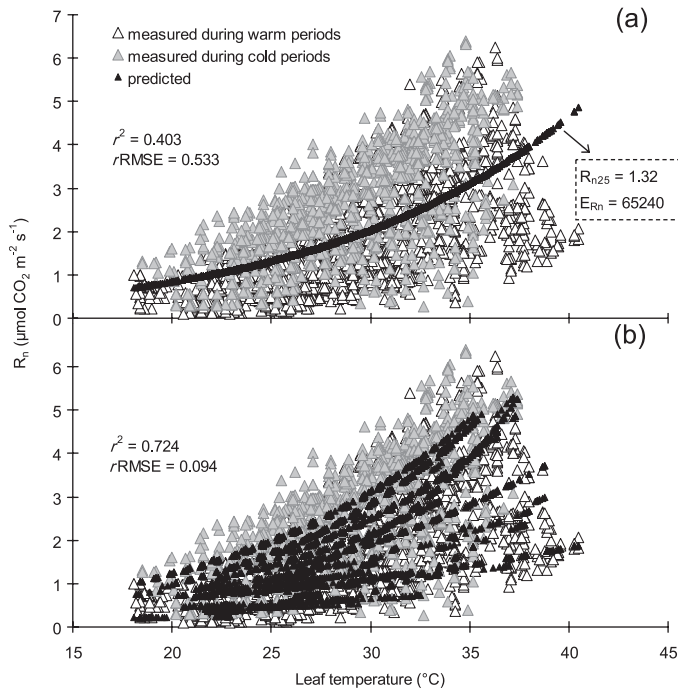


Fig. 4. Cynara's night respiration rates (R_n) in relation to leaf temperature. Data are presented per growth season and include leaves with various N_a . (a) The predicted R_n from a simple temperature-sensitive model (Equation 5; parameter values used are shown). (b) The predicted R_n from a combined nitrogen-, temperature-, and acclimation-sensitive model (see parameter values in Table 3).

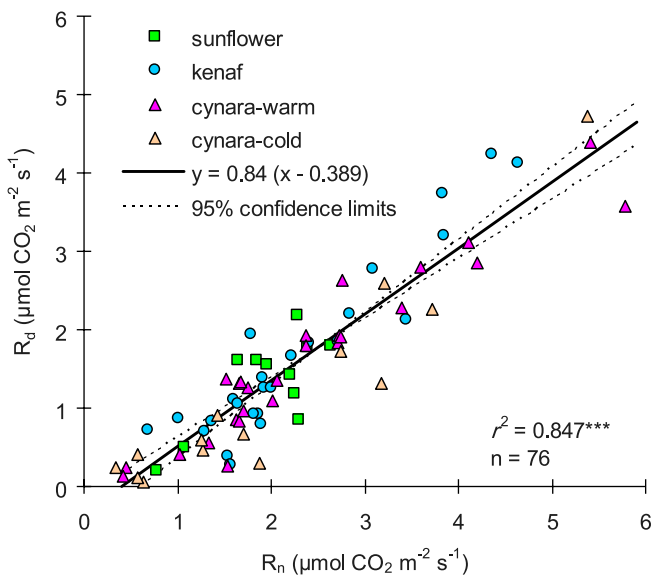


Fig. 5. Relationship between day (R_d) and night (R_n) respiration rates (see also Table 3 and Equation 12).

surprisingly, a maximum change was obtained in the estimated $V_{\text{cmax}25}$, whereas the remaining parameters were less affected (<5%; data not shown). Given that even the maximum change in V_{cmax} was $\sim 11\%$ in response to a 20% change, the parameter estimates were quite stable despite the uncertainties in values of Rubisco kinetic constants. A further analysis showed that the predicted A_n was sensitive

to a 20% decrease in χ_v and χ_j , whereas its sensitivity to other changes was weak (Fig. 9).

Lastly the models were validated against independent data sets (Fig. 10). Predictions versus observations for sunflower and kenaf were satisfactory ($r\text{RMSE} < 0.15$; Fig. 10a, b). For cynara the FvCB model was tested using measurements from a series of 24 h diurnal cycles (Fig. 10c), where stress conditions were unavoidably present (data sets outside the calibration range). In general, predictions were close to actual measurements, except for those data obtained from 14:00 h to 18:00 h, where a systematic overestimation was detected (Fig. 10c). The FvCB model responded to lowering temperature in late afternoon by increasing A_n ; however, actual measurements indicated that the photosynthetic apparatus could not recover so quickly from the 'photosynthesis midday depression'. The failure in predicting the depression and its after-effect during the recovery hours (Fig. 10c) might be attributed to the 'steady-state' character of the FvCB model. These results suggest that prediction of diurnal photosynthesis for species grown in the Mediterranean region requires more detailed approaches in which g_m , recovery functions for A_n (midday depression), and the effects of leaf water potential should be included (see Tuzet *et al.*, 2003; Vico and Porporato, 2008; Yin and Struik, 2009a).

Discussion

Use of A_n-I_{inc} curves to parameterize the FvCB model

The FvCB model parameters, J_{max} and V_{cmax} in particular, have been predominantly estimated from A_n-C_i data sets (Harley *et al.*, 1992; Medlyn *et al.*, 2002a). The value of A_n-C_i curves for parameterizing the FvCB model is confirmed (Fig. 2). It was also shown that V_{cmax} and J_{max} can be estimated sufficiently well by an appropriate analysis of A_n-I_{inc} data alone ($r^2=0.91-0.93$; Fig. 2). Unlike J_{max} , V_{cmax} cannot always be estimated from A_n-I_{inc} curves; that is when the entire curve is A_j limited (Fig. 1). This is often observed in field crops (e.g. cotton; Wise *et al.*, 2004). Actually, Boote and Pickering (1994) used only the A_j equation of the FvCB model to calculate leaf photosynthesis in their canopy photosynthesis model. For the purpose of using the complete FvCB model, the two-step approach is proposed to estimate both V_{cmax} and J_{max} from A_n-I_{inc} data. This is in line with the approach of Niinemets and Tenhunen (1997), but in contrast to that of Kosugi *et al.* (2003) and Müller *et al.* (2005) who assumed a fixed $J_{\text{max}}/V_{\text{cmax}}$ ratio of 2.1 at 25 $^{\circ}\text{C}$ (based on Wullschlegel, 1993) in their analyses. This assumption does not allow for the flexibility of the ratio as observed for different species or for the same species when grown under different environments, thereby introducing many uncertainties in parameter values (see Fig. 8 and discussion below).

The present results indicated that information from A_n-I_{inc} curves has been underexplored. Use of A_n-I_{inc} curves has an additional advantage in that data of A_n-C_i curves may be uncertain due to CO_2 leakage during gas exchange

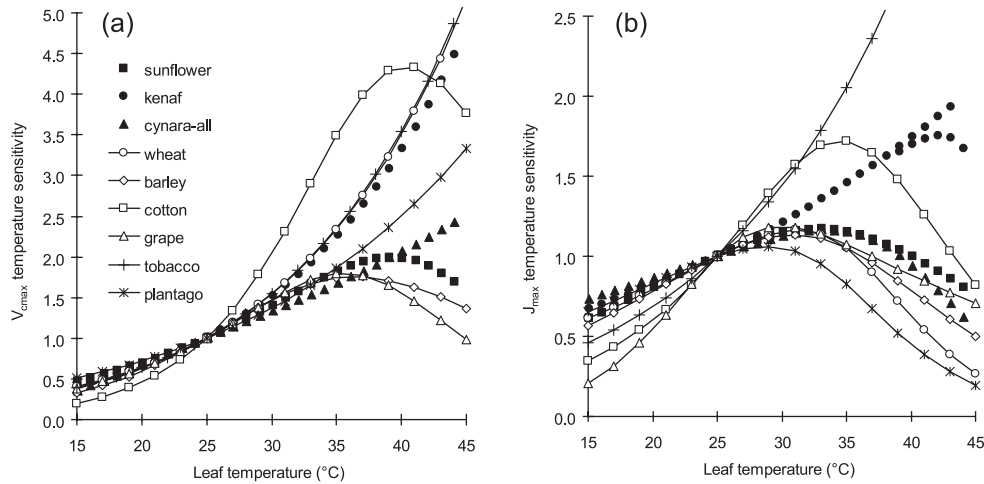


Fig. 6. Temperature sensitivities for V_{cmax} (a) and J_{max} (b). Values normalized to 1 at 25 °C. Filled symbols refer to bioenergy crops while open symbols refer to wheat (de Pury and Farquhar, 1997), barley (Braune *et al.*, 2009), cotton (Harley *et al.*, 1992), grapevine (Schultz, 2003), tobacco (Bernacchi *et al.*, 2001; 2003), and perennial *Plantago asiatica* (Ishikawa *et al.*, 2007). For kenaf, both observed J_{max} temperature sensitivities are plotted (see Table 3; note that for kenaf the measurement range was up to 41 °C).

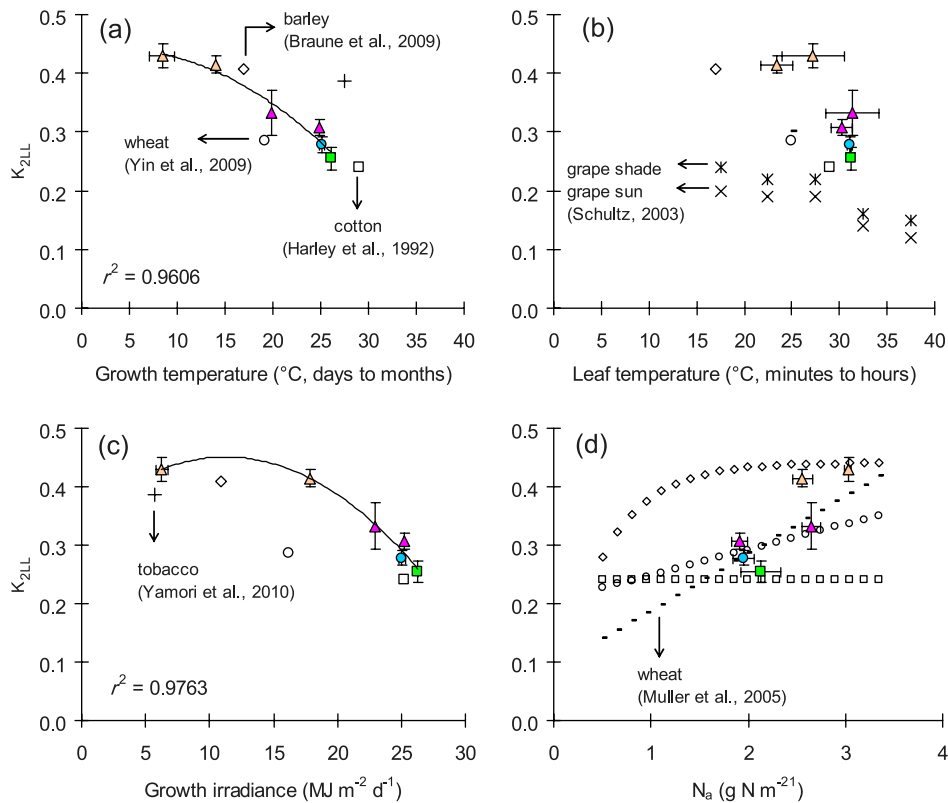


Fig. 7. Conversion efficiency of incident light into linear electron flux (κ_{2LL}) in relation to (a) seasonal growth temperature, (b) short-term changes in leaf temperature, (c) seasonal irradiance, and (d) N_a , for three bioenergy crops (filled symbols; see key in Fig. 5) and four major field crops (open symbols; see panels for details). Growth temperatures and irradiances were calculated from Supplementary Fig. S1 at *JXB* online. For sunflower and kenaf one average κ_{2LL} value (\pm vertical standard error) was calculated because measurements (set I) were conducted during the July–August period when temperature and radiation do not change much (Supplementary Fig. S1 at *JXB* online). In contrast, for cynara (cold and warm) four average κ_{2LL} values were calculated, reflecting the months November, April, May, and June, respectively. Horizontal bars (when larger than symbols) indicate the mean standard error of the explanatory variable. Information on growth temperature and irradiance could not be retrieved from the studies Müller *et al.* (2005) and Schultz (2003).

measurements when CO_2 set point values are either below or above the ambient air CO_2 level (Flexas *et al.*, 2007). Crop modellers used to measure $A_n - I_{inc}$ curves under an ambient

CO_2 condition, upon which an empirical model for light–response curves is parameterized. Provided that values of C_i across I_{inc} levels are properly monitored, re-analysing readily

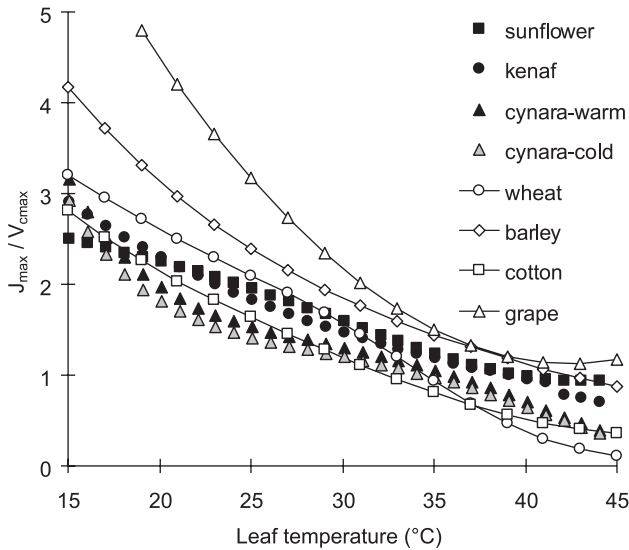


Fig. 8. $J_{\max}/V_{c\max}$ ratio versus leaf temperature. Closed symbols refer to bioenergy crops, open symbols to major field crops. Note that for cynara two lines were plotted because the parameter $J_{\max25}$ differs between seasons (see Equation 10 and Table 3).

available A_n-I_{inc} data to parameterize the FvCB model will strengthen photosynthesis calculations in crop models. This would expand the potential of combining classical photosynthetic data and the biochemical FvCB model to assess the impact of climate change on crop production and to examine options of bioenergy production under a changing climate.

On the other hand, caution should be exercised that use of A_n-I_{inc} data sets does not allow the model to account for the TPU (triose phosphate utilization)-limited rate, the third limitation added by Sharkey (1985) to the FvCB model. TPU limitation sets an upper limit to the maximum photosynthetic capacity and is usually observed at high CO_2 or/and low O_2 levels (e.g. Wise *et al.*, 2004), although many studies still ignore this limitation (e.g. Wohlfahrt *et al.*, 1999). The limitation, if it occurs, can be easily identified, at the high end of A_n-C_i curves, versus the Rubisco limitation that can be identified at the low end of A_n-C_i curves. In the present study, where essentially A_n-I_{inc} curves were used, it was not possible to detect this limitation, because both Rubisco and TPU limitations, if any, will occur at the high end of A_n-I_{inc} curves. This is certainly the disadvantage of using A_n-I_{inc} curves to parameterize the FvCB model. Fortunately, the present light response curves were obtained under ambient CO_2 conditions, so any TPU limitation, if it exists, can be assumed to be negligible under these measurement conditions. In the future climate where the ambient CO_2 level is expected to increase, the TPU limitation will be more likely to occur. Therefore, use of A_n-I_{inc} curves to estimate FvCB model parameters needs to be tested across high CO_2 levels and a broad range of other environmental variables in order to decide how conserved these parameters are.

Below the effects of temperature, N_a , and season on photosynthesis and respiration parameters, all derived from the current A_n-I_{inc} data for three bioenergy crops, are

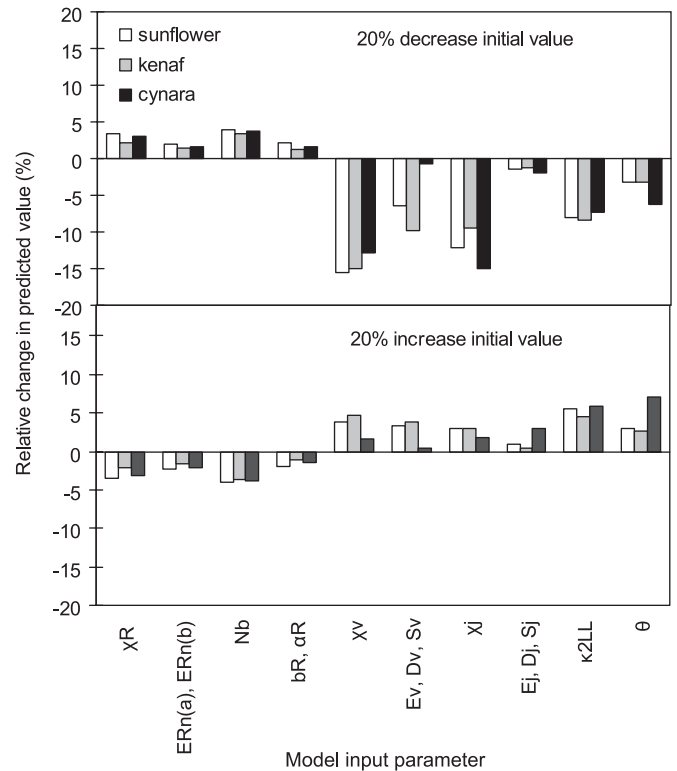


Fig. 9. Sensitivity analysis of the predicted A_n in response to a $\pm 20\%$ change in input parameter values for the photosynthesis model. The relative change in predicted value was calculated as: $100 \times (A_n, \text{predicted} - A_n, \text{predicted, original}) / A_n, \text{predicted, original}$. When input parameters were part of a linear or polynomial equation (e.g. E_j , D_j , S_j ; Equation 6) and strongly intercorrelated, a combined change was implemented.

discussed. The present findings will be compared with those reported for the crops wheat, barley, cotton, tobacco, and grapevine based on A_n-C_i or combined A_n-C_i and A_n-I_{inc} data sets, with attention to any conserved nature in these parameters among species.

Night and day respiration parameters: χ_{Rv} , $E_{Rn(a)}$, $E_{Rn(b)}$, b_{Rv} , and α_R

This study is among few in the literature providing direct R_n measurements, underlining the great importance of respiration in carbon budgets (Valentini *et al.*, 2000). The present estimates for χ_R (range: 0.61–0.95 $\mu\text{mol CO}_2 \text{ g}^{-1} \text{ N s}^{-1}$; Table 3) agree well with previous reports for crops (Hirose *et al.*, 1997; Reich *et al.*, 1998; Müller *et al.*, 2005; Braune *et al.*, 2009), but current values are almost double compared with those for trees (Bolstad *et al.*, 1999; Griffin *et al.*, 2002). The temperature sensitivity for respiration (E_{Rn}) was significantly correlated with N_a in all species (Equation 11; Table 3), indicating that respiration in leaves with high N_a values (young/sun leaves) was less sensitive to changes in temperature, while leaves with lower N_a values were more sensitive (senescence/shade leaves). Griffin *et al.* (2002) and Bolstad *et al.* (1999) working with tree leaves that were positioned in different canopy layers—also having different N_a values—found temperature sensitivities similar to those in the present study, while Turnbull *et al.*

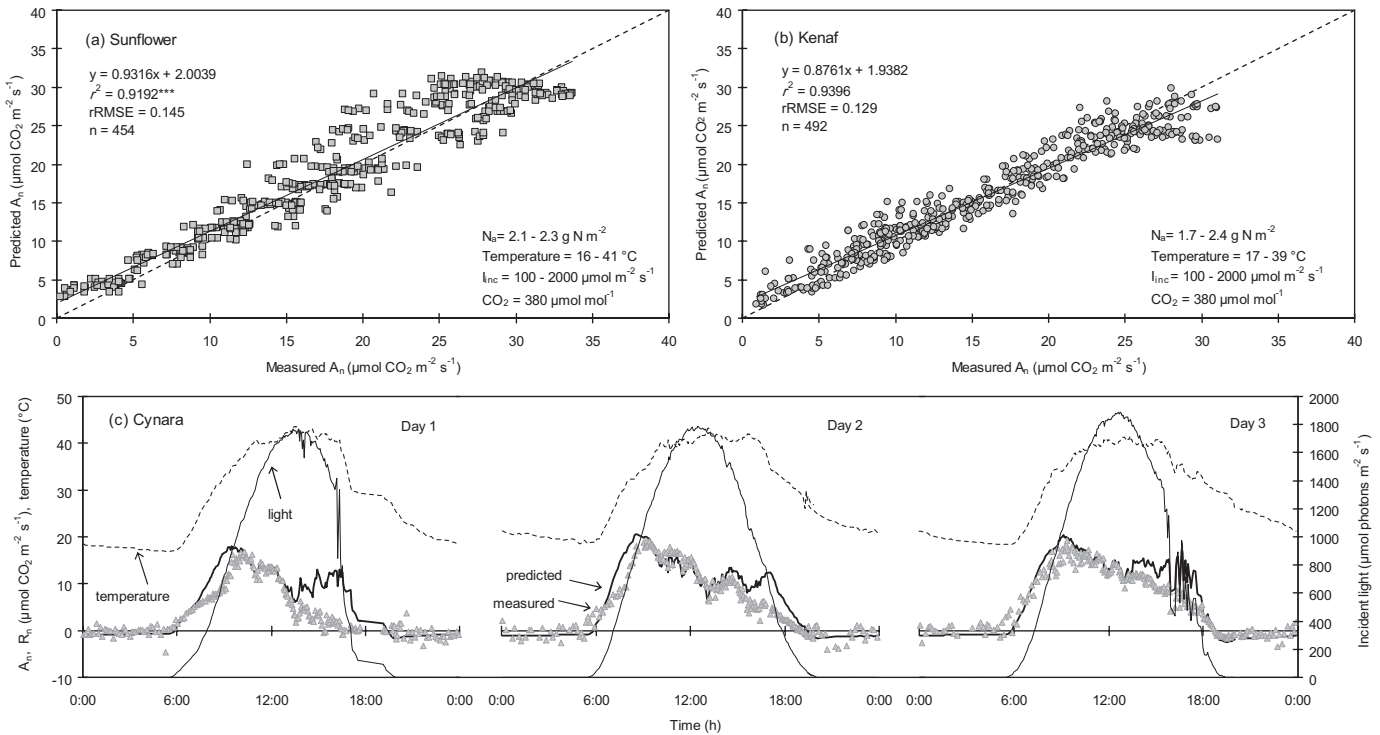


Fig. 10. Measured versus predicted photosynthesis (all panels) and measured versus predicted night respiration (only in the lower panel c). In c, canopy CO_2 varied from 350–380 $\mu\text{mol mol}^{-1}$ during day time to 450–600 $\mu\text{mol mol}^{-1}$ during night-time; VPD followed temperature variations, and stomatal conductance ranged from 0.05 $\text{mol m}^{-2} \text{ s}^{-1}$ during the night up to 0.48 $\text{mol m}^{-2} \text{ s}^{-1}$ during the day time. The model predicted diurnal trends moderately ($r^2=0.814$, $rRMSE=0.553$, $n=720$). When midday measurements were excluded (14:00–16:00 h), the model fit was improved ($r^2=0.930$, $rRMSE=0.335$, $n=543$).

(2003) reported the opposite. However, in none of these studies was E_{Rn} significantly correlated with N_a .

For cotton, Harley *et al.* (1992) reported a simple temperature-sensitive R_n model for leaves with variable N_a . The present analysis indicated that it is useful to calculate both R_n components as a function of N_a (e.g. Fig. 4; across all species, r^2 scaled from 0.53 to 0.77). The component R_{n25} accounted for 27% and E_{Rn} for the other 5% of this improvement in r^2 . However, the remaining unexplained variability in night data sets (see r^2 in Table 3; Fig. 4) means that apart from N_a , other factors should be explored.

Unlike for R_n , it is difficult to measure R_d directly as such measurements require sophisticated methodologies (e.g. Haupt-Herting *et al.*, 2001; Pinelli and Loreto, 2003; Pärnik and Keerberg, 2007). Its value is empirically estimated indirectly using various methods (for a comparison see Yin *et al.*, 2011), or is commonly fixed as 1% of V_{cmax} or as 50% of R_n (de Purry and Farquhar, 1997; Wohlfahrt *et al.*, 1998; Medlyn *et al.*, 2002a; Kosugi *et al.*, 2003; Braune *et al.*, 2009). Here, application of the Kok method (Sharp *et al.*, 1984) indicated a 28% reduction in R_d compared with R_n , an estimate which is positioned at the lowest reported range (light inhibition range: 24–90%; Buckley and Adams, 2011, and references therein).

Rubisco and electron transport parameters: N_b , χ_v , χ_j , κ_{2LL} , θ , E_v , E_j , D_v , and D_j

The present findings for N_b (Fig. 3) along with published data support the idea that this threshold value for photosyn-

thesis is not affected by temperature (Sage and Pearcy, 1987; Makino *et al.*, 1994; Niinemets and Tenhunen, 1997), CO_2 (Harley *et al.*, 1992; Hirose *et al.*, 1997), or irradiance levels (Makino *et al.*, 1997). Excluding the statistical bias that usually exists in N_b estimations (see the Materials and methods) it is believed that a common N_b is 0.3–0.4 g N m^{-2} for C_3 crop species (excluding legume crops; Supplementary Table S1 at *JXB* online). For use in modelling, it was shown that a $\pm 20\%$ change in the N_b value resulted in a $< 5\%$ change in the predicted A_n (Fig. 9).

The relationships between $A_{n,max}$ and N_a at near-optimum temperature ranges for sunflower, kenaf, and cynara (Fig. 3) agreed well with several non-legume C_3 species (Supplementary Fig. S2 at *JXB* online). The observed decline in $A_{n,max}$ at high temperature (Fig. 3; $N_a > 2 \text{ g N m}^{-2}$) is associated with g_m (Bernacchi *et al.*, 2002) and/or V_{cmax} and J_{max} limitations of photosynthesis (Fig. 6). N_a and leaf temperature explained $> 81\%$ of the temporal (seasonal) and spatial (within a crop canopy) variation in $A_{n,max}$ values (Fig. 3). The remaining unexplained variability might be due to leaf adaptation to different microenvironments created by CO_2 and light gradients within crop stands (Buchmann and Ehlinger, 1998; Archontoulis *et al.*, 2011). This may have an additional impact on J_{max} and V_{cmax} estimates and their ratio.

Nevertheless, the observed consistency among $A_{n,max}$ – N_a plots (Supplementary Fig. S2 at *JXB* online) along with the similar χ_v estimates for sunflower, kenaf, cynara, cotton, wheat, and barley (range: 60–82 $\mu\text{mol CO}_2 \text{ g}^{-1} \text{ N s}^{-1}$; Table 3;

Harley *et al.*, 1992; de Pury and Farquhar, 1997; Müller *et al.*, 2005, 2008; Braune *et al.*, 2009) suggests that χ_v is very conserved for this plant group ($A_{n,max}=30\text{--}35 \mu\text{mol CO}_2 \text{ m}^{-2} \text{ s}^{-1}$; Supplementary Fig. S2).

Unlike χ_v , χ_j for the same group was highly variable (90–165 $\mu\text{mol e}^- \text{ g}^{-1} \text{ N s}^{-1}$). However, the parameter χ_j (which determines J_{max25} ; Equation 10) is not independent of, but interrelated to, the values of κ_{2LL} and θ (see Equation 4). This means that use of constant κ_{2LL} and θ values across species and environments will bias J_{max} estimates and therefore the J_{max}/V_{cmax} ratio. Among sunflower, kenaf, and cynara, χ_j varied by 36%, κ_{2LL} by 39%, and θ by 28%, but in different directions (Table 3). When κ_{2LL} was fixed to 0.3 and θ to 0.7 (commonly assumed values; de Pury and Farquhar, 1997; Medlyn *et al.*, 2002a), the χ_j variation among crops and growing environments became smaller (15%), and the J_{max}/V_{cmax} ratio less variable.

The present analysis showed that variation in the electron transport rate among bioenergy crops followed changes in environmental conditions during growth (Supplementary Fig. S1 at *JXB* online), with higher J rates for cynara in low light ($<700 \mu\text{mol m}^{-2} \text{ s}^{-1}$; winter period) and higher J rates for sunflower and kenaf in high light conditions ($>700 \mu\text{mol m}^{-2} \text{ s}^{-1}$; summer period; Table 3, Equation 4). This is consistent with recent findings for tobacco (Yamori *et al.*, 2010) where plants grown under low light enhanced the efficiency of light acquisition while those grown under high light enhanced the capacity of light utilization, through changes in chlorophyll contents, the chlorophyll *alb* ratio, and cytochrome *f* and Rubisco contents.

In studies of Wullschleger (1993), Dreyer *et al.* (2001), and Medlyn *et al.* (2002a) the κ_{2LL} was fixed as a constant at 0.18, 0.24, and 0.30, respectively, across species, crop stages, and environments. However, Yin *et al.* (2009) directly demonstrated a positive relationship between κ_{2LL} and N_a , which was confirmed by the results of a model curve-fitting procedure (Müller *et al.*, 2005; Braune *et al.*, 2009; Yamori *et al.*, 2010).

In Fig. 7, κ_{2LL} information for eight crops is summarized and this large variation is interpreted in the light of long- or short-term response to temperature or irradiance. Across species, the highest κ_{2LL} values were found in crops grown under long-term low irradiance and temperature conditions (Fig. 7a, c). To understand this, it is necessary to underline the components of the κ_{2LL} parameter (see Equation A3 derived by Yin *et al.*, 2004, 2009; Yin and Struik, 2009a; also see equation 6 in Niinemets and Tenhunen, 1997). The fraction of I_{inc} absorbed by the leaf photosynthetic pigments (parameter β in Equation A3) is affected by long-term changes in light and temperature through its changes in leaf morphology. Leaves grown at high temperature are generally thinner, with a lower ability to absorb light (Poorter and Evans, 1998; Yamori *et al.*, 2005), therefore providing a reasonable explanation for the observed κ_{2LL} reduction with increasing temperature. On the other hand, leaves grown at high irradiance are thicker (Niinemets and Tenhunen, 1997), indicating that κ_{2LL} variation is much more complex and still not fully understood. Nonetheless,

caution should be exercised when modelling canopy photosynthesis based on the sun/shade approach (de Pury and Farquhar, 1997; Yin and van Laar, 2005) because κ_{2LL} increases with increasing N_a (Fig. 7d), while κ_{2LL} also increases with decreasing light (Schultz, 2003; shade leaves which generally have low N_a values; Fig. 7b).

The normalized temperature functions of V_{cmax} and J_{max} were variable across crops (Fig. 6), particularly above 30 °C, in line with Leuning (2002). This mean that the assumption used in crop modelling, a unique A_n response to temperature across crop species, is inappropriate when photosynthesis is calculated by the FvCB model. In the case of no available data, it is suggested that researchers as a first approximation use V_{cmax} and J_{max} temperature parameters from species that belong to the same family (see Fig. 6; cotton and kenaf belong to Malvaceae; sunflower and cynara to Asteraceae).

The J_{max}/V_{cmax} ratio provides an estimate of the relative activities of RuBP regeneration and Rubisco carboxylation, and incorporates both temperature and N_a effects. This study confirms (Table 3) the generally reported J_{max}/V_{cmax} value of 2.0 ± 0.5 (Wullschleger, 1993; Poorter and Evans, 1998; Bunce, 2000; Leuning, 2002; Medlyn *et al.*, 2002a). However, this ratio should not be considered constant in absolute terms. V_{cmax} is dependent on the Rubisco parameters used (up to 11% change; see also Medlyn *et al.*, 2002a) and J_{max} is affected by the assumed κ_{2LL} and θ values used (see earlier discussion). For instance, grape showed a much higher J_{max}/V_{cmax} ratio compared with other crops (Fig. 8). Apart from the effect of species, there are two possible artefacts causing this: the different Rubisco parameters used in that study (Schultz, 2003) and the lower grape κ_{2LL} values compared with the other crops (Fig. 7b). Also use of C_i instead of C_c affects this ratio. Thus approaches (e.g. Kosugi *et al.*, 2003; Müller *et al.*, 2005) that fix the J_{max}/V_{cmax} ratio at a constant value to parameterize the FvCB model should receive critical reservation.

Seasonal effects on photosynthesis and respiration in cynara

Direct interpretation of the seasonal effects on A_n and R_n for cynara is difficult because both the climate (Supplementary Fig. S1 at *JXB* online) and the plant stage are different, with new and old leaves being present (Archontoulis *et al.*, 2010a; Searle *et al.*, 2011). R_n acclimated to cold and warm environments to a larger extent than did A_n (Table 3; Fig. 4). This is consistent with previous studies (Yamori *et al.*, 2005; Ow *et al.*, 2008; Silim *et al.*, 2010).

The nature of R_n acclimation is variable within and among plant species, and it is usually related to changes in E_{Rn} and/or to changes in R_{n25} (Atkin *et al.*, 2005; Searle *et al.*, 2011). Given that χ_R did not change between seasons ($P=0.269$; Table 3) and that the measured winter leaves had higher N_a values than the summer leaves (on average 2.48 versus 1.53 g N m^{-2} ; see also Fig. 7d), this indicates that basal capacity, R_{n25} , plays an important role in this acclimation. Secondly, E_{Rn} was also higher during winter

periods. Apparently, cynara follows an ‘acclimation type II’ (Atkin *et al.*, 2005) where the overall elevation of the R_n –temperature response was affected by season and growth stage (Fig. 4).

Among FvCB parameters analysed, seasonal effects were found on two electron transport parameters, χ_j and κ_{2LL} (Table 3 and earlier discussion), and none related to V_{cmax} . Literature information on A_n acclimation is diverse among studies (Wilson *et al.*, 2000; Medlyn *et al.*, 2002a; Bernacchi *et al.*, 2003; Hikosaka, 2005; Yamori *et al.*, 2005; Braune *et al.*, 2009; Silim *et al.*, 2010). As far as is known, only Wilson *et al.* (2000) reported both χ_j and χ_v seasonal changes in trees, while Braune *et al.* (2009) found only χ_j variation for barley as in the present study. For cynara, the normalized V_{cmax} and J_{max} temperature functions were slightly changed between seasons, in line with other field studies (Medlyn *et al.*, 2002b; Schultz, 2003), but in contrast to growth chamber studies (Bernacchi *et al.*, 2003; Yamori *et al.*, 2005; Ishikawa *et al.*, 2007; Braune *et al.*, 2009) where plants were grown only at different temperatures. The fact that this study assessed leaves with different N_a status may be a reason, but an inconsistency between actual field and controlled chamber studies is obvious.

The J_{max}/V_{cmax} ratio has been reported to be either sensitive or insensitive to growth temperature (see discussion by Hikosaka *et al.*, 2005), growth irradiance (Poorter and Evans, 1998; Yamori *et al.*, 2010), and seasonal changes (Bunce, 2000; Medlyn *et al.*, 2002b). The present results suggest that cynara regulates the balance between RuBP regeneration and Rubisco carboxylation to maintain the J_{max}/V_{cmax} ratio almost constant (change <8%; Table 3) across seasons and growth stages.

Conclusions

This study provides new information on photosynthesis and respiration rates for three bioenergy crops, sunflower, kenaf, and cynara. It provides an alternative way to parameterize the FvCB model from A_n – I_{inc} data, instead of using A_n – C_i data that are more expensive to obtain. It was shown that major FvCB model parameters, V_{cmax} and J_{max} , derived from either A_n – C_i or A_n – I_{inc} analysis, are very close ($r^2=0.92$). Present models can predict photosynthesis under varying levels of C_i , I_{inc} , temperature, and leaf nitrogen, and can estimate night respiration under varying levels of temperature and leaf nitrogen, for the three bioenergy crops. Comparisons of FvCB model parameters among sunflower, kenaf, cynara, cotton, wheat, barley, tobacco, and grapevine indicated that only a few parameters were conserved. This means that in order to feed crop models properly, species-specific FvCB model parameters are needed. In this context, readily available A_n – I_{inc} data—that have been underexplored—can assist in that respect. By combining classical photosynthetic data and the biochemical model, the potential of crop growth models to assess the impact of climate change on crop production and to examine options of bioenergy production under a changing

climate is enlarged. Further research is needed to quantify reliably the effects of photosynthetic acclimation and diurnal midday depression identified in this study.

Supplementary data

Supplementary data are available at *JXB* online.

Figure S1. Average monthly temperatures, radiation, and precipitation at the experimental site (period: 2007–2009). Sunflower measurements were taken from July to August; kenaf measurements from July to September, and cynara measurements from November to June.

Figure S2. Reported relationships between light-saturated net assimilation rate at ambient CO_2 concentration and at near-optimum temperature ($A_{n,max}$ in $\mu mol CO_2 m^{-2} s^{-1}$) and leaf nitrogen content ($g N m^{-2}$) for C_3 crops (a), C_3 legume crops and trees (b), and C_4 crops (c). (d) An average relationship for C_3 and C_4 crops.

Table S1. Reported N_b values (minimum leaf nitrogen for photosynthesis, in $g N m^{-2}$) for various species.

Acknowledgements

SVA acknowledges financial support received from the Crop Physiology group (Wageningen University) and the Laboratory of Agronomy and Applied Crop Physiology (University of Thessaly) to accomplish this research, which is part of his PhD study. XY and PCS partly contributed to this research through their participation in the Dutch photosynthesis research programme BioSolar Cells, funded by the Ministry of Economic Affairs, Agriculture and Innovation.

Appendix

1. Estimating the optimum temperature from the peaked Arrhenius equation

The optimum temperature for V_{cmax} or J_{max} in Equation 6 is given by the following equation (Medlyn *et al.*, 2002a):

$$T_{opt} = \frac{D_x}{S_x - R \cdot \ln\left(\frac{E_x}{D_x - E_x}\right)} \quad (A1)$$

2. The relationship between κ_{2LL} and Φ_{CO2LL}

By dividing both parts of Equation 3 by I_{inc} and re-arranging, the efficiency of incident light conversion into e^- , κ_{2LL} , can be calculated mathematically from Φ_{CO2LL} :

$$\begin{aligned} \Phi_{CO2LL} &= \frac{A_n + R_d}{I_{inc}} \Big|_{I_{inc} \rightarrow 0} = \kappa_{2LL} \frac{C_i - \Gamma_*}{4C_i + 8\Gamma_*} \\ \Leftrightarrow \kappa_{2LL} &= \Phi_{CO2LL} \frac{4C_i + 8\Gamma_*}{C_i - \Gamma_*} \end{aligned} \quad (A2)$$

This approach was also used by Niinemets *et al.* (2001), but lacks any further interpretation.

3. Components of parameter κ_{2LL}

Yin *et al.* (2004) described a generalized stoichiometric equation for A_j , where the linear photosystem II (PSII) electron transport rate (J) was replaced by the total electron transport rate passing PSII (J_2) and fractions of the total e^- flux passing PSI that follow cyclic (f_{cyc}) and pseudocyclic (f_{pseudo}) pathways. Again, under low light conditions, dividing J by I_{inc} yields κ_{2LL} as follows (Yin and Struik, 2009a; Yin *et al.*, 2009):

$$\kappa_{2LL} = \frac{J}{I_{inc}} \Big|_{I_{inc} \rightarrow 0} = \frac{J_2}{I_{inc}} \left(1 - \frac{f_{pseudo}}{1 - f_{cyc}} \right) = \rho_2 \beta \Phi_{2LL} \left(1 - \frac{f_{pseudo}}{1 - f_{cyc}} \right) \quad (A3)$$

By definition, the variable J_2 can be replaced by the term $\rho_2 \times \beta \times \Phi_{2LL} \times I_{inc}$, where ρ_2 is the fraction of absorbed irradiance partitioned to PSII (usually assumed to be 0.5), β is the fraction of I_{inc} absorbed by the leaf photosynthetic pigments, and Φ_{2LL} is the PSII e^- transport efficiency under limiting light.

References

- Atkin OK, Bruhn D, Hurry VM, Tjoelker MG.** 2005. The hot and the cold: unravelling the variable response of plant respiration to temperature. *Functional Plant Biology* **32**, 87–105.
- Archontoulis SV, Struik PC, Vos J, Danalatos NG.** 2010a. Phenological growth stages of *Cynara cardunculus*: codification and description according to the BBCH scale. *Annals of Applied Biology* **156**, 253–270.
- Archontoulis SV, Struik PC, Yin X, Bastiaans L, Vos J, Danalatos NG.** 2010b. Inflorescence characteristics, seed composition, and allometric relationships predicting seed yields in the biomass crop *Cynara cardunculus*. *Global Change Biology–Bioenergy* **2**, 113–129.
- Archontoulis SV, Vos J, Yin X, Bastiaans L, Danalatos NG, Struik PC.** 2011. Temporal dynamics of light and nitrogen vertical distributions in canopies of sunflower, kenaf and cynara. *Field Crops Research* **122**, 186–198.
- Beringer T, Lucht W, Schaphoff S.** 2011. Bioenergy production potential of global biomass plantations under environmental and agricultural constraints. *GCB Bioenergy* **3**, 299–312.
- Bernacchi CJ, Pimentel C, Long SP.** 2003. *In vivo* temperature response functions of parameters required to model RuBP-limited photosynthesis. *Plant, Cell and Environment* **26**, 1419–1430.
- Bernacchi CJ, Portis AR, Nakano H, von Caemmerer S, Long SP.** 2002. Temperature response of mesophyll conductance. Implications for the determination of Rubisco enzyme kinetics and for limitations to photosynthesis *in vivo*. *Plant Physiology* **130**, 1992–1998.
- Bernacchi CJ, Singaas EL, Pimentel C, Portis AR, Long SP.** 2001. Improved temperature response functions for models of Rubisco-limited photosynthesis. *Plant, Cell and Environment* **24**, 253–259.
- Bolstad PV, Mitchell K, Vose JM.** 1999. Foliar temperature–respiration response functions for broad-leaved tree species in southern Appalachians. *Tree Physiology* **19**, 871–878.
- Boote KJ, Pickering NB.** 1994. Modelling photosynthesis of row crop canopies. *HortScience* **29**, 1423–1434.
- Braune H, Müller J, Diepenbrock W.** 2009. Integrating effects of leaf nitrogen, age, and growth temperature into the photosynthesis–stomatal conductance model LEAFC3-N parameterized for barley (*Hordeum vulgare* L.). *Ecological Modelling* **220**, 1599–1612.
- Buchmann N, Ehlinger JR.** 1998. CO₂ concentration profiles, and carbon and oxygen isotopes in C₃ and C₄ crop canopies. *Agricultural and Forest Meteorology* **89**, 45–58.
- Buckley TN, Adams MA.** 2011. An analytical model of non-photorespiration CO₂ release in the light and dark in leaves of C3 species based on stoichiometric flux balance. *Plant, Cell and Environment* **34**, 89–112.
- Bunce JA.** 2000. Acclimation of photosynthesis to temperature in eight cool and warm climate herbaceous C3 species: temperature dependence of parameters of a biochemical photosynthesis model. *Photosynthesis Research* **63**, 59–67.
- Connor DJ, Hall AJ, Sadras VO.** 1993. Effects of nitrogen content on the photosynthetic characteristics of sunflower leaves. *Australian Journal of Plant Physiology* **20**, 251–263.
- Cosentino SL, Riggi E, D’Agosta G.** 2004. Leaf photosynthesis in kenaf (*Hibiscus cannabinus* L.) in response to water stress. In: *Proceedings of the 2nd World Biomass Conference*, Rome, Italy, 374–376.
- Danalatos NG, Archontoulis SV.** 2010. Growth and biomass productivity of kenaf (*Hibiscus cannabinus* L.) under different agricultural inputs and management practices in central Greece. *Industrial Crops and Products* **32**, 231–240.
- De Pury DGG, Farquhar GD.** 1997. Simple scaling of photosynthesis from leaves to canopies without the errors of the big-leaf models. *Plant, Cell and Environment* **20**, 537–557.
- Dreyer E, Le Roux X, Montpied P, Daudet AF, Masson F.** 2001. Temperature response of leaf photosynthetic capacity in seedlings from seven temperate tree species. *Tree Physiology* **21**, 223–232.
- Either GJ, Livingston NJ.** 2004. On the need to incorporate sensitivity to CO₂ transfer conductance into the Farquhar–von Caemmerer–Berry leaf photosynthesis model. *Plant, Cell and Environment* **27**, 137–153.
- Evers JB, Vos J, Yin X, Romero P, van der Putten PEL, Struik PC.** 2010. Simulation of wheat growth and development based on organ-level photosynthesis and assimilate allocation. *Journal of Experimental Botany* **61**, 2203–2216.
- Farquhar GD, von Caemmerer S.** 1982. Modelling of photosynthetic response to environmental conditions. In: Lange OL, Nobel PS, Osmond CB, Ziegler H, eds. *Physiological plant ecology II. Water relations and carbon assimilation. Encyclopaedia of plant physiology, New Series*, Vol. 12 B. Berlin: Springer Verlag, 549–588.
- Farquhar GD, von Caemmerer S, Berry JA.** 1980. A biochemical model of photosynthetic CO₂ assimilation in leaves of C₃ species. *Planta* **149**, 78–90.
- Flexas J, Diaz-Espejo A, Berry JA, Cifre J, Galmes J, Kaldenhoff R, Medrano H, Ribas-Carbo M.** 2007. Analysis of leakage in IRGA’s leaf chambers of open gas exchange systems: quantification and its effects in photosynthesis parameterization. *Journal of Experimental Botany* **58**, 1533–1543.

- Flexas J, Ribas-Carbó M, Diaz-Espejo A, Galmes J, Medrano H.** 2008. Mesophyll conductance to CO₂: current knowledge and future prospects. *Plant, Cell and Environment* **31**, 602–621.
- Galmes J, Medrano H, Flexas J.** 2007. Photosynthetic limitation in response to water stress and recovery in Mediterranean plants with different growth forms. *New Phytologist* **175**, 81–93.
- Goudriaan J.** 1979. A family of saturation type curves, especially in relation to photosynthesis. *Annals of Botany* **43**, 783–785.
- Goudriaan J, van Laar HH.** 1994. *Modelling potential crop growth processes*. Dordrecht, The Netherlands: Kluwer Academic Publishers.
- Griffin KL, Turnbull M, Murthy R.** 2002. Canopy position affects the temperature response of leaf respiration in *Populus deltoides*. *New Phytologist* **154**, 609–619.
- Gu L, Pallardy SG, Tu K, Law BE, Wullschlegel SD.** 2010. Reliable estimation of biochemical parameters from C3 leaf photosynthesis–intercellular carbon dioxide response curves. *Plant, Cell and Environment* **33**, 1852–1874.
- Harley PC, Thomas RB, Reynolds JF, Strain BR.** 1992. Modelling photosynthesis of cotton grown in elevated CO₂. *Plant, Cell and Environment* **15**, 271–282.
- Haupt-Herting S, Klug K, Fock HP.** 2001. A new approach to measure gross CO₂ fluxes in leaves. Gross CO₂ assimilation, photorespiration, and mitochondrial respiration in the light in tomato under drought stress. *Plant Physiology* **126**, 388–396.
- Hikosaka K.** 2005. Nitrogen partitioning in the photosynthetic apparatus of *Plantago asiatica* leaves grown under different temperature and light conditions: similarities and differences between temperature and light acclimation. *Plant and Cell Physiology* **46**, 1283–1290.
- Hirose T, Ackerly DD, Traw MB, Ramseier D, Bazz FA.** 1997. CO₂ elevation, canopy photosynthesis and optimal leaf area index. *Ecology* **78**, 2339–2350.
- Ishikawa K, Onoda Y, Hikosaka K.** 2007. Intraspecific variation in temperature dependence of gas exchange characteristics among *Plantago asiatica* ecotypes from different temperature regimes. *New Phytologist* **176**, 356–364.
- Kosugi Y, Shibata S, Kobashi S.** 2003. Parameterization of the CO₂ and H₂O gas exchange of several temperate deciduous broadleaved trees at the leaf scale considering seasonal changes. *Plant, Cell and Environment* **26**, 285–301.
- Leuning R.** 2002. Temperature dependence of two parameters in a photosynthetic model. *Plant, Cell and Environment* **25**, 1205–1210.
- Makino A, Nakano H, Mae T.** 1994. Effects of growth temperature on the responses of ribulose-1,5-bisphosphate carboxylase, electron transport components, and sucrose synthesis enzymes to leaf nitrogen in rice, and their relationships to photosynthesis. *Plant Physiology* **105**, 1231–1238.
- Makino A, Sato T, Nakano H, Mae T.** 1997. Leaf photosynthesis, plant growth and nitrogen allocation in rice under different irradiances. *Planta* **203**, 390–398.
- Medlyn BE, Dreyer E, Ellsworth D, et al.** 2002a. Temperature response of parameters of a biochemically based model of photosynthesis. II. A review of experimental data. *Plant, Cell and Environment* **25**, 1167–1179.
- Medlyn BE, Loustau D, Delzon S.** 2002b. Temperature response of parameters of a biochemically based model of photosynthesis. I. Seasonal changes in mature maritime pine (*Pinus pinaster* Alt.). *Plant, Cell and Environment* **25**, 1155–1165.
- Muchow RC.** 1990. Effects of leaf nitrogen and water regime on the photosynthetic capacity of kenaf (*Hibiscus cannabinus*) under field conditions. *Australian Journal of Agricultural Research* **41**, 845–852.
- Müller J, Wernecke P, Diepenbrock W.** 2005. LEAFC3-N: a nitrogen sensitive extension of the CO₂ and H₂O gas exchange model LEAFC3 parameterized and tested for winter wheat (*Triticum aestivum* L.). *Ecological Modelling* **183**, 183–210.
- Müller J, Braune H, Diepenbrock W.** 2008. Photosynthesis–stomatal conductance model LEAFC3-N: specification for barley, generalised nitrogen relations and aspects of model application. *Functional Plant Biology* **35**, 797–810.
- Niinemets U, Ellsworth D, Lukjanova A, Tobias M.** 2001. Site fertility and the morphological and photosynthetic acclimation of *Pinus sylvestris* needles to light. *Tree Physiology* **21**, 1231–1244.
- Niinemets U, Tenhunen JD.** 1997. A model separating leaf structural and physiological effects on carbon gain along light gradients for the shade-tolerant species *Acer saccharum*. *Plant, Cell and Environment* **20**, 845–865.
- Ow FL, Griffin KL, Whitehead D, Walcroft AS, Turnbull M.** 2008. Thermal acclimation of leaf respiration but not photosynthesis in *Populus deltoides* × *nigra*. *New Phytologist* **178**, 123–134.
- Pärnik T, Keerberg O.** 2007. Advanced radiogasometric method for the determination of the rates of photorespiratory and respiratory decarboxylations of primary and stored photosynthates under steady state photosynthesis. *Physiologia Plantarum* **129**, 33–44.
- Pinelli P, Loreto F.** 2003. ¹²CO₂ emission from different metabolic pathways measured in illuminated and darkened C3 and C4 leaves at low, atmospheric and elevated CO₂ concentration. *Journal of Experimental Botany* **54**, 1761–1769.
- Pons TL, Flexas J, von Caemmerer S, Evans JR, Genty B, Ribas-Carbo M, Bruynoli E.** 2009. Estimating mesophyll conductance to CO₂: methodology, potential errors, and recommendations. *Journal of Experimental Botany* **60**, 2217–2234.
- Pons TL, Welschen RAM.** 2002. Overestimation of respiration rates in commercially available clamp-on leaf chambers. Complications with measurement of net photosynthesis. *Plant, Cell and Environment* **25**, 1367–1372.
- Poorter H, Evans JR.** 1998. Photosynthetic nitrogen-use efficiency of species that differ inherently in specific leaf area. *Oecologia* **116**, 26–37.
- Reich PB, Walters MB, Ellsworth DS, Vose JM, Volin JC, Gresham C, Bowman WD.** 1998. Relationships of leaf dark respiration to leaf nitrogen, specific leaf area and leaf life-span: a test across biomes and functional groups. *Oecologia* **114**, 471–482.
- Sage RF, Rearcy RW.** 1987. The nitrogen use efficiency of C₃ and C₄ plants. II. Leaf nitrogen effects on the gas exchange characteristics of *Chenopodium album* L. and *Amaranthus retroflexus* L. *Plant Physiology* **84**, 959–963.
- Searle SY, Thomas S, Griffin KL, Horron T, Kornfeld, Yakir D, Hurry V, Turnbull MH.** 2011. Leaf respiration and alternative oxidase

in field-grown alpine grasses respond to natural changes in temperature and light. *New Phytologist* **189**, 1027–1039.

Schultz HR. 2003. Extension of a Farquhar model for limitation of leaf photosynthesis induced by light environment, phenology and leaf age in grapevines (*Vitis vinifera* cv. White Riesling and Zinfandel). *Functional Plant Biology* **30**, 673–687.

Sharkey TD. 1985. Photosynthesis in intact leaves of C₃ plants: physics, physiology and rate limitations. *Botanical Review* **51**, 53–105.

Sharkey TD, Bernacchi CJ, Farquhar GD, Singass EL. 2007. Fitting photosynthetic carbon dioxide response curves for C₃ leaves. *Plant, Cell and Environment* **30**, 1035–1040.

Sharp RE, Matthews MA, Boyer JS. 1984. Kok effect and the quantum yield of photosynthesis. Light partially inhibits dark respiration. *Plant Physiology* **75**, 95–101.

Silim SN, Ryan N, Kubien DS. 2010. Temperature of photosynthesis and respiration in *Populus balsamifera* L.: acclimation versus adaptation. *Photosynthesis Research* **104**, 19–30.

Sinclair TR, Horie T. 1989. Leaf nitrogen, photosynthesis, and crop radiation use efficiency: a review. *Crop Science* **29**, 90–98.

Tuzet A, Perrier A, Leuning R. 2003. A coupled model of stomatal conductance, photosynthesis and transpiration. *Plant, Cell and Environment* **26**, 1097–1116.

Turnbull MH, Whitehead D, Tissue DT, Schuster WSF, Brown KL, Griffin KL. 2003. Scaling foliar respiration in two contrasting forest canopies. *Functional Ecology* **17**, 101–114.

Valentini R, Matteucci G, Dolman AJ, et al. 2000. Respiration as the main determinant of carbon balance in European forests. *Nature* **404**, 861–865.

Vico G, Porporato A. 2008. Modelling C₃ and C₄ photosynthesis under water-stressed conditions. *Plant and Soil* **313**, 187–203.

von Caemmerer S, Farquhar GD. 1981. Some relationships between the biochemistry of photosynthesis and the gas exchange of leaves. *Planta* **153**, 376–387.

von Caemmerer S, Farquhar G, Berry J. 2009. Biochemical model of C₃ photosynthesis. In: Laisk A, Nebal L, Govindjee, eds. *Photosynthesis in silico: understanding complexity from molecules to ecosystems*. Dordrecht: Springer Science+Business Media B.V., 209–230.

Warren CR. 2004. The photosynthetic limitation posed by internal conductance to CO₂ movement is increased by nutrient supply. *Journal of Experimental Botany* **55**, 2313–2321.

Wilson KB, Baldocchi DD, Hanson PJ. 2000. Spatial and seasonal variability of photosynthetic parameters and their relationship to leaf nitrogen in a deciduous forest. *Tree Physiology* **20**, 565–578.

Wise RR, Olson AJ, Schrader SM, Sharkey TD. 2004. Electron transport is the functional limitation of photosynthesis in field-grown

Pima cotton plants at high temperature. *Plant, Cell and Environment* **27**, 717–724.

Wohlfahrt G, Bahn M, Horak I, Tappeiner U, Cerbusca A. 1998. A nitrogen sensitive model of leaf carbon dioxide and water vapour gas exchange: application to 13 key species from differently managed mountain grassland ecosystems. *Ecological Modelling* **113**, 179–199.

Wohlfahrt G, Bahn M, Haufner E, Horak I, Michaeler W, Rottmar K, Tappeiner U, Cerbusca A. 1999. Inter-specific variation of the biochemical limitation to photosynthesis and related leaf traits of 30 species from mountain grassland ecosystems under different land use. *Plant, Cell and Environment* **22**, 1281–1296.

Wullschlegler SD. 1993. Biochemical limitations to carbon assimilation in C₃ plants—a retrospective analysis of the A/C_i curves from 109 species. *Journal of Experimental Botany* **44**, 907–920.

Yamori W, Evans JR, von Caemmerer S. 2010. Effects of growth and measurement light intensities on temperature dependence of CO₂ assimilation rate in tobacco leaves. *Plant, Cell and Environment* **33**, 332–343.

Yamori W, Noguchi K, Terashima I. 2005. Temperature acclimation of photosynthesis in spinach leaves: analyses of photosynthetic components and temperature dependencies of photosynthetic partial reactions. *Plant, Cell and Environment* **28**, 536–547.

Yin X, van Oijen M, Schapendonk AHCM. 2004. Extension of a biochemical model for the generalized stoichiometry of electron transport limited C₃ photosynthesis. *Plant, Cell and Environment* **27**, 1211–1222.

Yin X, Struik PC. 2009a. C₃ and C₄ photosynthesis models: an overview from the perspective of crop modelling. *NJAS–Wageningen Journal of Life Sciences* **57**, 27–38.

Yin X, Struik PC. 2009b. Theoretical reconsiderations when estimating the mesophyll conductance to CO₂ diffusion in leaves of C₃ plants by analysis of combined gas exchange and chlorophyll fluorescence measurements. *Plant, Cell and Environment* **32**, 1513–1524.

Yin X, Struik PC, Romero P, Harbinson J, Evers JB, van den Putten PEL, Vos J. 2009. Using combined measurements of gas exchange and chlorophyll fluorescence to estimate parameters of a biochemical C₃ photosynthesis model: a critical appraisal and a new integrated approach applied to leaves in a wheat (*Triticum aestivum*) canopy. *Plant, Cell and Environment* **32**, 448–464.

Yin X, Sun Z, Struik PC, Gu J. 2011. Evaluating a new method to estimate the rate of leaf respiration in the light by analysis of combined gas exchange and chlorophyll fluorescence measurements. *Journal of Experimental Botany* **62**, 3489–3499.

Yin X, van Laar HH. 2005. *Crop systems dynamics: an ecophysiological simulation model for genotype-by-environment interactions*. Wageningen, The Netherlands: Wageningen Academic Publishers.